INTEGRATIVE PROCESSING IN THE HUMAN CEREBRAL CORTEX FOLLOWING MULTI- AND UNI-MODAL STIMULATION: MAGNETOENCEPHALOGRAPHIC STUDIES

Khanh Lam

Doctor of Philosophy

Department of Physiological Sciences,

School of Life Sciences,

The Graduate University for Advanced Studies

and

Department of Integrative Physiology,

National Institute for Physiological Sciences

Okazaki, Aichi, 444-8585

JAPAN

1999

CONTENTS

1. Abbreviations

MEG	Magnetoencephalography
EEG	Electroencephalography
EOG	Electrooculography
fMRI	Functional magnetic resonance imaging
PET	Positron emission tomography
CT	Computer-assisted X-ray tomography
RCBF	Regional cerebral blood flow
SQUID	Superconductive quantum interference device
S1	Primary somatosensory cortex
S2	Secondary somatosensory cortex
M1	Primary motor cortex
V1	Primary visual cortex
V2	Visual area 2
V3	Visual area 3
V4	Visual area 4
V5	Visual area 5
A1	Primary auditory cortex
PO	Parieto-occipital area
MT	Middle temporal area
MST	Medial superior temporal area
MSTd	Dorsomedial part of the MST
STS	Superior temporal sulcus
PA points	Preauricular points
SEP	Somatosensory evoked potential
SEF	Somatosensory evoked magnetic field
EPSP	Excitatory post-synaptic potential
RMS	Root mean square
ECD	Equivalent current dipole
RDK	Random dot kinematogram
ANOVA	Analysis of variance

2. Abstract

The human cortex can be divided into many distinct functional regions, such as the primary somatosensory cortex (S1) and the primary visual cortex (V1). Most of the remaining regions are known as association areas; they respond in a more complicated way to external stimuli. For a better understanding of this complexity we investigated the integrative processing of the human cerebral cortex following multi- and uni-modal stimulation by using magnetoencephalography (MEG).

In the first study, in order to elucidate the mechanisms underlying the neural process to detect multi-modal stimulation (somatosensory, visual and auditory), we recorded somatosensory evoked magnetic fields (SEFs) following electrical stimulation of the median nerve with continuous visual (cartoon or random dot motion) or auditory (music) interference in 12 normal subjects. Random dot motion included random and coherent motions of the dots. In the hemisphere contralateral to the stimulated nerve, the middle-latency components (35-60 ms in latency) were significantly enhanced by visual, but not by auditory stimulation. The dipoles of all components within 60-70 ms following stimulation were estimated to be very close to each other, around the hand area of the S1. In the ipsilateral hemisphere, the middle-latency components (70-100 ms in latency), the dipoles of which were estimated to be in the secondary somatosensory cortex (S2), were markedly decreased in amplitude by both the visual and auditory stimulation. These changes in waveforms by visual and auditory stimulation are thought to be due to the effects of the activation of polymodal neurons, which receive not only somatosensory but also visual and/or auditory inputs, in areas 5 and/or 7 as well as in the medial

superior temporal area (MST) and superior temporal sulcus (STS), although a change of attention might also be a factor causing such findings.

In the second study, in order to understand the neural process to detect uni-modal stimulation with different features in one specific functional (visual) system we investigated the magnetic response of the human extrastriate cortex in detection of coherent and random motions.

Although the direction selectivity is a cardinal property of the neurons in the visual motion detection system, recent studies have showed that the motion of numerous elements without global direction (random motion) activates the human and monkey visual system the same as does coherent motion which has a global direction. We used MEG to investigate whether these two motions are processed in distinct neural subsystems with five subjects. Both motions were created by a random dot kinematogram (RDK) with three speeds (0.6, 9.6, and 25° s^{-1}) and used to evoke magnetic responses from the human extrastriate cortex. Response latencies to the simple onset of coherent motion were affected by the speed, whereas those for random motion were not. The estimated origin of the response to coherent motion onset was located lateral (median: 0.7 cm) to that for random motion. Responses to change from coherent to random motion and vise versa differed from those to the simple onset and offset of coherent motion in terms of latencies and estimated origins. Response amplitudes were similar under all stimulus conditions. These findings indicate that the response to random motion is not due to nonspecific activation of the coherent motion detection system but support the view that the human visual system has a subsystem for the process of random motion different from that for coherent motion. We consider that the presence of the subsystem to detect random motion increases the detectability of coherent motion in the visual

scene of random motion.

In conclusion, using MEG we could assess the temporal and the spatial properties of the magnetic responses of the human cerebral cortex to multi-modal as well as uni-modal stimulation. With high spatial and temporal resolution, MEG seemed to be the best method available to investigate the complicated neural process in restricted areas.

3. Introduction

The present thesis includes two research works. The first is on the effects of visual and auditory stimulation on somatosensory evoked magnetic fields (SEFs) and the second, the response of the human extrastriate cortex in detection of coherent and random motions.

3.1. Motivation for the two studies

The human cortex can be divided into many distinct functional regions, such as primary somatosensory cortex (S1), which receives somatosensory stimuli, is located posterior to the Rolandic fissure. The area in the frontal lobe just anterior to the Rolandic fissure contains neurons concerned with integration of muscular activity: each site of the primary motor cortex (M1) is involved in the movement of a specific part of the body. S1 and M1 on the left side of the brain monitor and control the right side of the body and vice versa. The primary auditory cortex (A1) is in the temporal lobe buried within the Sylvian fissure, while the primary visual cortex (V1) is in the occipital lobe at the back of the head. Most of the remaining regions are known as association areas; they respond in a more complicated way to external stimuli. In the monkey, Brodmann's areas 5 and 7 in the parietal lobe and the cortex buried in the superior temporal sulcus (STS) receive convergent projections from cortical somatosensory, visual, and auditory areas, and are anatomically considered a sensory convergence areas (Jones and Powell, 1970; Neal et al., 1987, 1990; Pandya and Seltzer, 1982; Pearson and Powell, 1985). Physiologically, it has been demonstrated that these areas are polysensory regions because neurons in such areas respond not only to somatosensory stimuli but also to other kinds of stimuli

such as visual and auditory stimulation (Bruce et al., 1981; Hari et al., 1990; Hyvarinen, 1981; Hyvarinen and Poranen, 1974; Leinonen et al., 1979; Leinonen and Nyman, 1979). We therefore suspect that the integrative processing of various kinds of sensations, such as somatosensory, visual and auditory stimulation, also take place in these areas in the human brain. When we use multi-modal stimulation (somatosensory, visual and auditory), the neural process to detect these kinds of stimuli may take place in the polysensory areas. To investigate such a complicated processing, researchers usually use uni-modal stimulation as the control and multi-modal stimulation as the test condition. In our experimental design, somatosensory stimulation was chosen to be the control condition because the neural processes in the somatosensory system are understood much better than those in other systems. Visual or auditory together with somatosensory stimulation was selected for the multi-modal conditions. For evaluating the effect of multi-modal stimulation on the brain responses, we compared the responses in these two conditions, sought the difference between them and explained what neural process and what brain area corresponds to these changes. In the second experiment, we concentrated on the responses of only one specific functional region of the brain (the visual motion areas in the human extrastriate cortex) to the uni-modal stimulation with different features. A cluster of physiological and anatomical studies using monkey and psychological studies on the functions of the visual motion areas allows us easily to compare our results with theirs.

To establish 'where' and 'when' the neural processes to detect multi-modal (somatosensory, visual and auditory) and uni-modal (coherent and random motions of dots) stimulation take place, we needed a technique that had enough temporal resolution to show the arrival of signals in the cortex, and enough spatial resolution

to be able to distinguish the activation of different cortical areas. The only technique with adequate spatiotemporal resolution is magnetoencephalography (MEG), with the exception of those which use intracortical electrodes.

3.2. Advantages and disadvantages of MEG comparing with other imaging techniques

Modern imaging techniques provide high-resolution images through which structure and metabolism of the human brain can be studied in vivo. Computer-assisted X-ray tomography (CT) and magnetic resonance imaging (MRI) produce high-quality but static maps of the brain anatomy. Functional information about the brain on a time scale of minutes can be obtained with regional cerebral blood flow (RCBF), positron emission tomography (PET) and functional MRI (fMRI) measurements, based on changes in cell metabolism. Functional imaging has a relatively limited temporal resolution and the subject is exposed to x rays, to radioactive tracers, or to time-varying and strong static magnetic fields. There are only two totally nonivasive techniques to study the actual brain function on a millisecond scale: Electroencephalography (EEG) and MEG. Sensory signals from the thalamus arrive at the superficial and deep sites of pyramidal neurons in the cerebral cortex which are considered to generate EEG and MEG (thalamo-cortical projection). The superficial thalamo-cortical projection generates excitatory post-synaptic potentials (EPSP) in the superficial site of the pyramidal neurons. EPSP in turn generate both intracellular and extracellular currents (Ii and Io). Ii is the main contributor for generating MEG and EEG. In other words, the magnetic field recorded from the human brain is considered to represent the spatiotemporal summation of intracellular currents produced by the excitatory post-synaptic potentials for more than a million pyramidal neurons (Hamalainen et al. 1993,

Okada et al. 1997).

EEG, employed for about 60 years, involves the measurement of the electric potential distribution by means of electrodes attached to the scalp. The biggest disadvantage of EEG is its poor spatial resolution. There are three layers between the brain and the EEG electrodes on the scalp: cerebrospinal fluid, bone (scalp) and skin. Their electrical conductivity is different and therefore the boundaries between these three structures distort the pattern of the current. That means electric activities generated in the brain are significantly affected by these three layers, and it is difficult for us to know the exact activation area in detail by analyzing EEG. In contrast, magnetic fields are not affected by these layers. In MEG, the minute (50-500 fT) magnetic fields, produced by the same brain events as in EEG, are detected outside the head with SQUID (Superconductive Quantum Interference Device) magnetometers. By mapping the magnetic field distribution outside the head, the sites of neural events can be located with an accuracy of a few millimeters and the temporal evolution of the activation can be traced with a millisecond resolution. Thus, MEG seems to be the best method available to investigate complicated interactions in restricted areas such as interference effects (Kakigi et al., 1995, 1996, 1997).

The disadvantage of MEG is that only dipoles oriented parallel to the cortex (tangential) can be detected. In other words, dipoles generated in the sulcus are main distributors for generating MEG. A radially oriented dipole produces very weak magnetic fields. In theory, in a homogeneous sphere it should produce no magnetic field outside the sphere. MEG is very sensitive to the magnetic fields generated in the superficial areas, but not in the deep areas. Therefore, in MEG, one is usually concerned with the upper most layer of the brain, the cerebral cortex, which is a 2-4 mm thick sheet of gray tissue.

4. The effects of visual and auditory stimulation on SEF

4.1. Motivation

Somatosensory evoked brain responses following electrical stimulation of the peripheral nerves in humans are markedly modified by various types of somatomotor interference such as tactile stimulation or movement applied to various parts of the human body. Many investigators have studied these interference effects by analyzing the averaged EEG, in other words, somatosensory evoked electroencephalogram (SEP) (Lee and White, 1974; Abbruzzese et al., 1981; Rushton et al., 1981; Jones, 1981; Jone and Power, 1984; Kakigi and Jones, 1985, 1986; Kakigi, 1986; Cohen and Starr, 1987; Cheron and Borenstein, 1991, 1992; Touge et al., 1997), but the mechanisms and the sites responsible for interference effects have not been elucidated. Several other studies have investigated these interference effects using MEG (Rossini et al.,1989; Kakigi et al., 1995, 1996, 1997; Naka et al. 1998). However, to our knowledge, there has been no study regarding the effects of visual or auditory stimulation on SEF.

4.2. Background

4.2.1. SEF following electrical median nerve stimulation

In the hemisphere contralateral to the stimulated median nerve, three different kinds of deflections were identified. Main deflections, N20m-P30m-N40m-P60m, and their counterparts, P20m-N30m-P40m-N60m, were clearly identified in this hemisphere. Their equivalent current dipoles (ECDs) are located around the hand area of S1 and oriented anteroposteriorly. Therefore, area 3b, which is located on the posterior bank of the central sulcus, was considered to be the generator of

these deflections, as suggested by studies of SEP (see Allison et al., 1989a, b) and of SEF (Hari et al., 1984; Wood et al., 1985). Restricted deflections, P25m and N25m, were considered to be generated in area 1 in S1. The middle-latency deflections, N90m-P90m were considered to be generated in the secondary somatosensory cortex (S2). From the hemisphere ipsilateral to the stimulated median nerve, small N90m-P90m, the dipoles of which were estimated to be in S2, were identified.

4.2.2. SEF following electrical median nerve stimulation with somatomotor interference

Using MEG, most studies on the interference effect have examined brain responses following upper limb stimulation and the results of two have close relation with ours. Kakigi et al. (1995) investigated the interference effects caused by active finger movements on SEF following electrical stimulation of the median nerve in seven normal subjects and reported the short-latency cortical deflections, N20m-P20m, P30m-N30m and P25m-N35m were significantly attenuated with no latency changes. In contrast, the following middle-latency deflections, the N40m-P40m and the P60m-N60m were clearly changed in terms of latency and duration by the interference. They considered that the interference effects on all deflections took place in the hemisphere contralateral to the stimulated median nerve, because all of the equivalent current dipoles (ECDs) of the short- and the middle-latency deflections in the "control", "interference" and "difference" waveforms were located there. The interference effects on the short-latency deflections were suggested to be due to the interactions between the neurons in areas 1 and 3b, which were activated by sensory inputs from cutaneous mechanoreceptors, and the neurons in area 3a which were activated by sensory inputs from the muscle spindles. The interference

effects on the middle-latency deflections may mainly be due to the excitations of neurons in area 4 caused by either continuous movement-related activities or by sensory inputs spreading from the sensory cortex.

There is an another study worthy of mention. Kakigi et al. (1996) investigated the effects of tactile interference stimulation on somatosensory evoked magnetic fields following electrical stimulation of the median nerve in eight normal subjects and reported when stimulation was applied to the hand ipsilateral to the stimulated nerve, only the third response (3M) was enhanced in five subjects, but other responses were attenuated in all subjects. These interference effects were probably due to interactions in areas 1 and 3b. After stimulation of the contralateral hand, only the second response (2M) was enhanced in six subjects. This effect was probably due to the intracerebral interactions mediated through the corpus callosum.

There have also been studies of the interference effect following peripheral nerve stimulation from the lower limb (Kakigi et al. 1997; Naka et al., 1998).

4.3. Objective

The objective of the first study was to analyze the effects of visual and auditory stimulation on SEF following electrical stimulation of the median nerve to elucidate the underlying mechanisms of interactions in the human cerebral cortex.

4.4. Subjects and methods

We studied twelve normal male and female volunteers who ranged in age from 26 to 48 (mean age 33.9). Each gave informed consent for participation in this study, which was first approved by the Ethical Committee at our Institute. The visual

acuity of subjects was examined before the experiment, and was corrected with lenses when necessary.

The electric stimulus was a random voltage square-wave pulse delivered transcutaneously to the left median nerve at the wrist at a rate of 1 Hz. The stimulus duration was 0.5 ms, and the intensity was sufficient to produce a definite twitch of the thumb. The recording was made in a dark and calm magnetically shielded room (10 lux).

We used two different kinds of visual stimulation; a cartoon as the complicated stimulus and random dot motion as the simple stimulus. The cartoon was an animation video for children which included the three short stories of "The three little pigs", "The wolf and the seven little kids" and "The ugly duckling". This cartoon was projected on a screen (84 cm in width × 62 cm in height) inside the experiment room by a video projector (Barcodata 3100, Barco). A random dot kinematogram (RDK) generated by a VSG2/3 graphics board (Cambridge Research Systems) were projected on the same screen as that used for the cartoon. White dots (0.2 × 0.2°, 224cd m^{-2}, 200 per frame) on a dark background (4.3 cd m^{-2}) moving randomly and dots with horizontal coherent motion (25° s^{-1}) were presented alternately. This stimulation was used in our previous study (Kaneoke et al., 1997). Silence was maintained during both visual stimulation. For the auditory stimulus experiment, classical piano music from a CD (Chopin: The Waltzes) was used. All subjects reported being comfortable in both the visual and auditory stimulation experiments. To aid fixation during both visual and auditory stimulation we used a red laser spot (LP-110, Ser No.241692, Plus Corp., Japan), 4 mm in diameter, projected on the center of the same screen used for the visual stimulation. The distance between the subjects' nasion and the fixation spot was 1.3 m.

SEF was measured with dual 37-channel magnetometers (Magnes, Biomagnetic Technologies, San Diego, CA). The gradiometer was arranged in a uniformly distributed array in concentric circles over a spherically concave surface. The device was 144 mm in diameter. Each coil was 20 mm in diameter, and the centers of each coil were 22 mm apart. Each coil was connected to a SQUID. The center of the probe was placed around the C3 and C4 positions (according to the International 10-20 System), each covered the left and the right hemisphere, respectively. Data were filtered with a 0.1-200 Hz bandpass filter, and digitized at a sampling rate of 2083.3 Hz. The analysis time was 100 ms before and 400 ms after the stimulus, and the DC was offset using the pre-stimulus period as the baseline. Vertical and horizontal electrooculograms (EOGs) were used to monitor eye movements (bandpass: 0.1-30 Hz, sampling rate: 1,024 Hz). Epochs in which signal variations of larger than 3pT in magnetic response or 80μV in the EOG were excluded from averaging.

A spherical model was fitted to the digitized head shape of each subject (Sarvas, 1987), and the location (x, y, z positions) and orientation of a best-fitted single ECD were estimated for each time point (Fig. 22). The origin of the coordinate system is the midpoint between the left and right preauricular (PA) points. The positive X-axis extends from the origin through the nasion. The positive Z-axis extends from the origin through the top of the head, such that it is perpendicular to the plane formed by the nasion and both PA points. The positive Y-axis extends from the origin through the left PA. The correlation between the recorded measurements and the values obtained from the ECD estimate was calculated, to evaluate how closely the measured values corresponded to the theoretical field generated by the model. To avoid confusion, we used only a single ECD analysis in this study. For a strict

evaluation, we analyzed only the components whose isocontour maps indicated the presence of only one dipole, whose correlation value was over 0.97, and for which the calculated dipole was located in the cortex.

Four different sessions were held. 1. Control session: Left median nerve was stimulated and the subject simply looked at the red laser spot at the center of the screen with no other stimulation. 2. Cartoon session: Left median nerve was stimulated and the cartoon was shown on the screen while the subject looked at the red laser spot. 3. Random dots session (dots session): Left median nerve was stimulated and the random dot motion was shown on the screen while the subject looked at the red laser spot. 4. Music session: Left median nerve was stimulated and the music was played through a speaker while the subject looked at the red laser spot. The subjects were not asked to give their attention to any stimulus but to focus on the small red laser spot on the screen. The SEF was triggered not to the visual or auditory stimulation but to the electrical stimulation to the median nerve, i.e., these experiments were performed to determine the effects of continuous and concurrent visual or auditory stimulation on time-locked electrically-stimulated SEF. The order of the sessions was random, and two series of four sessions each were done. Two hundred trials were averaged in one session. When there was no significant difference between these two series, we adopted the grand-averaged waveforms ($2 \times 200 = 400$ averages) for the statistical analysis.

The change in two factors was analyzed: (1) Amplitude: A summation of magnetic fields of the maximum out- and in-going fluxes, and (2): A measure of the magnetic signal strength of the collected data. The maximum values of both amplitude and root mean square (RMS) for each recognizable component around the peak latency were measured. The changes in the amplitude and RMS for each

component between the control and each multi-modal stimulus condition and among the multi-modal stimulus conditions were analyzed using the paired t-test and two-factors analysis of variance (ANOVA). In the two-factors ANOVA, subjects and multi-modal stimulus conditions are factors in the experiment, and amplitude or RMS serves as the dependent variable. We did not calculate the dipole moment for the statistical analysis because at each time point it was variable and unstable in some sessions. The change in amplitude and RMS of each component in each session were calculated as percentages, with the amplitude and RMS of the control waveform set at 100%. For example, if the amplitudes of the 3M component in the control and cartoon session waveforms were 100 fT and 130 fT, respectively, the value of the cartoon session was 130%. To evaluate the changes in the dipole location under each multi-modal stimulus condition, the x, y and z values were also analyzed with the paired t-test and two-factors ANOVA.

MRI scans (Shimadzu Magnex 150 XT 1.5T, Shimadzu, Kyoto, Japan) were obtained for all subjects. The T1-weighted coronal, axial and sagittal images with continuous slices 1.5 mm in thickness were adopted for overlays with the ECD sources detected by MEG. The same anatomical landmarks used to create the MEG head-based three-dimensional (3D) coordinate system based on the location of the nasion and bilateral PA points were visualized in the MR images by affixing to these points with cod liver oil capsules (3 mm diameter). The MEG source locations were converted into pixels and slice values using the MRI transformation matrix and inserted onto the corresponding MRIs.

4.5. Results

4.5.1. Control waveforms

The SEF following median nerve stimulation in normal subjects have been described previously (Baumgartner et al., 1991; Huttunen et al., 1987; Tiihonen et al., 1989), and detailed results of SEF by using our gradiometer have been reported (Kakigi, 1994; Kakigi et al., 1995; 1996; Xiang et al., 1997). In the present study, four components were clearly identified in all subjects from the hemisphere contralateral to the stimulation, but interindividual differences existed in terms of latency and amplitude. The latencies of these components were about 16-20 ms (1M), 20-30 ms (2M), 35-45 ms (3M) and 45-60 ms (4M) (Figs. 1 and 2). A following long-latency component, 80-120 msec in latency, was also identified. In some subjects, peak latencies and amplitudes were variable, isocontour maps did not indicate a single dipole, their correlation values were below 0.97. We therefore did not analyze them in the present study. In the hemisphere ipsilateral to the stimulation, a large component, MI (magnetic fields in the ipsilateral hemisphere), was recorded in 7 of the 12 subjects, and was 70-100 msec in latency (Fig. 1).

4.5.2. Multi-modal waveforms

Some components were significantly changed in amplitude and RMS in the multi-modal stimulus conditions, although, there were some inter-individual differences (Table 1) (Figs. 3-5).

Contralateral hemisphere

At first, results were analyzed using the paired t-test. The first component (1M) and the second component (2M) were not significantly changed in terms of

latency, amplitude, RMS or location between the control and each multi-modal stimulus condition or among multi-modal stimulus conditions (Table 1) (Fig. 3). Regarding the third component (3M) (Figs. 3 and 4), there was a clear enhancement of both amplitude ($P<0.02$) and RMS ($P<0.05$) in the cartoon session as compared with the control session. In the dots session, the 3M amplitude ($P<0.05$) and RMS ($P<0.02$) were also significantly enhanced. In the music session, two subjects showed a remarkable enhancement of both amplitude and RMS but the others did not, and no significant change was identified. Among the three multi-modal stimulus conditions, the amplitude of the 3M in the dots session was significantly larger than that in the music session ($P<0.01$). Regarding the fourth component (4M) (Figs. 3 and 4), it was clearly enhanced in the cartoon session in both amplitude ($P<0.01$) and RMS ($P<0.001$), but was not significantly changed in the dots or music sessions as compared with the control session. Among the multi-modal stimulus conditions, there was also a significant enhancement of both amplitude ($P<0.05$) and RMS ($P<0.05$) in the cartoon session in comparison with the music session (Table 1).

Results were also analyzed using the two-way ANOVA (subjects, stimulus conditions). Regarding the 3M, there was a significant effect of multi-modal stimulation on amplitude ($P<0.02$) and RMS ($P<0.05$). Compared with the control session by the post-hoc comparisons, there was a clear enhancement of both amplitude ($P<0.01$) and RMS ($P<0.02$) of the 3M in the cartoon session. In the dots session, the 3M amplitude ($P<0.01$) and RMS ($P<0.01$) were also significantly enhanced. No significant change was found among the three multi-modal stimulus conditions. Regarding the 4M, there was also a significant effect of multi-modal stimulation on amplitude ($P<0.05$) but not on RMS. Compared with the control session, the 4M amplitude was clearly enhanced in the cartoon session ($P<0.02$), but

was not significantly changed in the dots or music sessions. Among the multi-modal stimulus conditions, there was a significant enhancement of amplitude in the cartoon session in comparison with the dots session ($P<0.02$) and the music session ($P<0.02$).

Ipsilateral hemisphere

The middle-latency component (MI) was attenuated in six out of seven subjects who showed a clear MI in three multi-modal stimulus conditions. There was a significant effect of multi-modal stimulation on the MI amplitude ($P<0.01$) using the two-factors ANOVA. This effect was statistically significant between the control and the cartoon session ($P<0.01$ by both paired t-test and ANOVA) and the music session ($P<0.02$ by paired t-test and $P<0.01$ by ANOVA) (Table 1) (Fig. 5).

Using the two-way ANOVA, it also showed that each multi-modal stimulus condition has different effect degrees on magnetic responses in different subjects ($P<0.001$).

4.5.3. Dipole locations

The ECDs of all four components in the control session as well as each multi-modal stimulus condition in all subjects were identified around the hand area of the S1 contralateral to the stimulated median nerve (Figs. 6-8). Differences in the x, y and z coordinates between the control and multi-modal stimulus condition were measured in each subject and analyzed by the paired t-test and two-way ANOVA (Table 2). Only the ECD of the 3M in the cartoon session was more posterior (1.5 mm on average) than that in the control session in 11 of the 12 subjects. Its difference was significant by the paired t-test ($P<0.01$) but not by ANOVA. The other

components' ECDs showed no significant difference.

The ECDs of the MI in the ipsilateral hemisphere were located around the superior bank of the Sylvian fissure, i.e., the S2, in the control and all three multi-modal stimulus conditions (Fig. 9). There was no significant change in the x, y or z coordinates between the control and multi-modal stimulus conditions (Table 2).

To summarize the results, the following four major findings were obtained:

1. The short latency-components, i.e., 1M and 2M, did not show any changes in any of the three multi-modal stimulus conditions.
2. There was a clear enhancement of the 3M and 4M components in the cartoon and/or dots sessions compared with the control session. The effects on the 4M component were more predominant in the cartoon session.
3. Music had no obvious effect on any of the four components from the hemisphere contralateral to the stimulation.
4. The middle-latency component in the ipsilateral hemisphere generated in the S2 was significantly attenuated in the cartoon and the music sessions.

4.6. Discussion

To our knowledge, there is no prior systematic study on the interaction between somatosensory and visual/auditory stimulation in humans, but important results in monkeys have been reported. Leinonen et al. (1979) studied neuronal activities in the lateral part of associative area 7 of the monkey, and reported that of 228 cells, 16% were visual, 40% were somesthetic and 14% were visual and somesthetic (bimodal). They also studied the anterolateral part of the area 7 associative face area (Leinonen and Nyman, 1979). They found that of 85 cells, 2% were visual, 26% were somesthetic and 33% were visual and somesthetic. Hyvarinen

and Poranen (1974), Hyvarinen (1981) also reported polymodal neurons in area 7.

In a study of the anterior bank of the caudal superior temporal sulcus of the temporal lobe, Hikosaka et al. (1988) divided this area into three subareas: The medial superior temporal region (MST), a mostly unresponsive region, and the caudal STS polysensory region (cSTP). Of 266 cells in the monkey MST, they found that 93% were visual and 7% were trimodal (somesthetic, visual and auditory). In the mostly unresponsive region, of 300 cells, 25% were visual. In the cSTP, of 200 cells, 30% were visual, 17% were auditory, 5% were somesthetic, 11% were visual and auditory, 4% were visual and somesthetic, 4% were auditory and somesthetic, and 2% were trimodal cells. Bruce et al. (1981) also reported polymodal neurons in the temporal lobe.

There is also some anatomical evidence for pathways between areas 5, 7 and S1 and/or S2 in the animals. Kazakov et al. (1981) reported the shape, size and localization of cells which make monosynaptic connections between the primary sensory areas and parietal cortex and the distribution of fiber terminals of such cells in the associative parietal cortex were determined. Narikashvili et al. (1977) found that, in unanesthetized immobilized cats, stimulation of the primary sensory areas (auditory or somatosensory) could elicit spindles in association cortex as well as in the stimulated area. This spindle, induced from the sensory areas, interacts with the spindles elicited by the direct electrical stimulation on the association cortex. Neal et al. (1987, 1990) reported area 7b is reciprocally and precisely connected with area 5, S2, area 23 of the cingulate cortex, the retroinsular area (Ri), the granular insular area (Ig), and with the cortex in the walls of the superior temporal sulcus. Between S1 and area 7b there are two sequences of connections in parallel with each other, one through area 5 and the other through S2. Pearson and Powell (1985) found in

the rhesus monkey that the degeneration after a small lesion in a representation in S1 virtually fills the representation in area 5 and there is extensive overlap of the degeneration after two lesions in widely separated parts of the representation in S1. Of the cytoarchitectonic subdivisions of S1, area 2 projects most heavily upon area 5 and area 3b the least, and there is a reversal in the antero-posterior dimension with more posterior parts of S1 projecting to more anterior parts of area 5. The corticocortical fibers from S1 end in layers III and IV of area 5, and while the degeneration in layer IV is continuous it is in distinct 'prongs' in layer III.

In the previous studies, some neurons responding to visual and/or auditory stimulation in parietal and temporal areas were found to be continuously excited during the experiments. By using the procedure described herein, we might thus be able to determine the effects of continuous neural activities in such areas on the time-locked somatosensory evoked brain responses generated in the S1 and S2.

The isocontour maps and high correlation values of all five components in the control and each multi-modal stimulus condition indicated a single dipole, and the estimated ECDs were located around the hand area of the S1 contralateral to the stimulation and the S2 ipsilateral to the stimulation. Although the 3M location in the cartoon session was significantly posterior compared to that in the control session, its short distance, only 1.5 mm on average, could not be meaningfully evaluated. There was no significant effect of multi-modal stimulation on the short-latency components, 1M and 2M. This finding suggests that the primary responses generated just after the ascending signals reach the S1 are not affected by the continuous excitation of polymodal neurons in areas 5 and/or 7.

In contrast, the 3M and 4M components were significantly enhanced by visual stimulation, but not by auditory stimulation. The 3M waveforms were almost the

same in the cartoon and dots sessions, whereas the 4M component was only affected by the cartoon stimulus. Since music did not cause a significant change, the simple effect of a change of attention must be a small factor. As mentioned earlier, we asked the subjects to give their close attention to the red laser spot on the center of the screen during the experiment.

By other modalities of sensorimotor interference such as tactile stimulation or movement, all components were previously observed to be reduced in amplitude, probably due to activity generated in S1 which inhibited the activity of cortical responses to somatosensory stimulation. In contrast, the 3M and 4M components were enhanced in amplitude when the present subjects watched the visual stimulation. One possibility to account for this phenomenon is the reduction of inhibitory effects on the S1 by areas 5 and/or 7. That is, neuronal activities in response to somatosensory stimulation in some neurons in areas 5 and/or 7 usually inhibit cortical responses to somatosensory stimulation in the S1. However, such inhibitory effects may be reduced by simultaneous visual stimulation, because a relatively large number of neurons respond to both somatosensory and visual stimulation. Due to this interaction caused by visual and somatosensory stimulation, the inhibitory effects on cortical activities in the S1 may be reduced, enhancing the middle-latency components. It is also possible that the activities in the polymodal neurons in areas 5/7 may simply enhance the activities in the S1. Another possibility is that both somatosensory and visual stimulation activated polymodal cells in S1, even though until now there are no reports about this kind of cells in S1 in the human cerebral cortex. The last possibility is that the 3M and 4M may be hybrid components of activities in area 3b in S1 and areas 5 and/or 7, unlike the short-latency components 1M and 2M. In such a case, enhanced activities in areas 5 and/or

7 make their amplitudes larger.

For the 3M, two subjects did not follow the group trend in the music session. They showed a remarkable enhancement of both amplitude and RMS (Fig. 4). This variability may be explained by different sensitivity to music in each subject.

It is difficult to account for the reason why only the middle-latency components, 3M and 4M, were enhanced. Desmedt et al. (1983) reported that the middle-latency cortical components of SEP approximately 25-60 msec in latency were affected by paying an attention to an electrical stimulation in an oddball paradigm, but the short-latency components were not changed. Since the present subjects paid close attention to the red light spot rather than the electrical stimulation (which was opposite to the paradigm reported by Desmedt et al., 1983), we do not consider the attention focus to be the main reason. The generating mechanisms of the middle-latency cortical components may be more complicated, including various factors such as vulnerability to the effects from surrounding areas as shown in the present study, compared with the short-latency cortical components.

The effect of the cartoon was almost the same as that of the random dots on the 3M component, but it was larger on the 4M component. Since the cartoon is a more complicated visual stimulation in terms of color, shape, etc. than the random dots, it may stimulate a larger number of visual cells in polysensory areas than do the random dots. This finding is also consistent with previous reports that different visual stimuli and different colors do not have equal effects on visual cells (Komatsu, 1993; Komatsu et al., 1996).

The marked inhibition of the component generated in the S2 of the hemisphere ipsilateral to the stimulation, caused by not only visual but also auditory stimulation, was a quite interesting finding. Attention to the somatosensory stimulation (Hari et

al., 1990) and imagining the movement of a stimulated limb without actual moving it (movement imagery) (Kakigi et al., 1997) caused marked enhancement of S2 responses, in contrast to the present findings. Therefore, close attention to visual and auditory stimulation may account for the present results, although we asked the subjects to give their continuous attention to the red laser spot on the screen. Another possibility is that polymodal neurons in the MST and/or STS cause such phenomenon, although the polymodal neurons in areas 5 and/or 7 may cause an enhancement of components rather than the inhibition shown in the present study. A continuous activation of neurons in the auditory cortex may account for part of this phenomenon, but this hypothesis does not explain the effects of visual stimulation. The last possibility is that reduced amplitude occurred due to a change in the underlying current distribution. The interference effect might change dipole direction such that the radical components increased and tangential components decreased, although dipole direction in each session was similar to each other.

5. Response of the human extrastriate cortex in detection of coherent and random motions

5.1. Motivation:

Humans perceive the overall direction of motion made up of numerous erroneously moving elements, even though each element's motion does not represent that direction at any moment. Random dot kinematograms have been used in human and monkey experiments (Morgan and Ward, 1980; Siegel and Andersen, 1988) to clarify the mechanisms that underlies detection of such global motion. One of the most striking facts found is that humans and monkeys at best can detect the direction in which only a few percent of the dots are moving coherently, remaining dots moving randomly (Newsome and Pare, 1988; Baker, Jr. et al., 1991). To detect such coherent dot motion in the background of randomly moving dots, each dot's motion must first be detected locally then integrated in a large spatial scale (Williams and Sekuler, 1984). This integration may be done in the extrastriate cortex because the middle temporal area (MT/V5) in the monkey is reported to be specifically related to the motion process (Maunsell and Van Essen, 1983; Zeki, 1974) and the neurons' receptive field is larger than the V1 (Van Essen et al., 1981) which is related more to detection of the local motion of each dot (Snowden et al., 1991). Certainly, MT neurons in monkeys are closely related to the perception of coherent motion (Newsome et al., 1989; Salzman et al., 1990).

If the extraction of the coherent motion from the scene of many randomly moving dots is the major role of the visual system, then random dot motion is a "noise" for the visual system (Baker et al., 1991; Croner and Albright, 1999; Scase et al., 1996). A recent human study using PET (McKeefry et al., 1997), however,

showed that the same cortical regions such as V1 and the secondary visual cortex (V2) and V5 were similarly activated to both coherent and random motions. The result apparently contradicts the idea that neurons in V5 are heavily implicated in the detection of coherent motion rather than random motion because of their receptive fields and directionally tuned responsibility. Thus, the visual system may have a distinct subsystem to analyze random motion. If so, the detection of random dot motion must be mediated by a neural process different from that for coherent motion. This is because if locally detected motion of randomly moving dots is integrated in the same way as coherent motion, it would produce a null direction that is the same as that of stationary dots randomly plotted. We hypothesize that the coherent and the random motions are processed in the same cortical regions but that their underlying neural processes differ.

In a previous MEG study, we found that random dot motion evoked magnetic responses from the human extrastriate cortex (Kaneoke et al., 1997). The results motivated us to examine this hypothesis using MEG which may elucidate properties of responses from the extrastriate cortex that a PET study could not measure owing to its low temporal and spatial resolutions (McKeefry et al., 1997).

5.2. Background

5.2.1. The neural pathway of the visual motion perception

The lateral geniculate nucleus (LGN) of the thalamus receives the output of retinal ganglion cells before projecting to the striate cortex. The lateral geniculate nucleus contains six layers of cells. Four of these have quite small cells (parvocellular) and receive information from small retinal ganglion cells. The other two layers have larger cells (magnocellular) and receive information from the larger

retinal ganglion cells. The main projection of the lateral geniculate nucleus is into layer 4c of the striate cortex; the P-pathway connects to layer 4cβ and the M-pathway to layer 4cα (Hubel and Wiesel, 1972). Layer 4cα projects to layer 4b, which in turn is known to project directly to area MT (Shipp and Zeki, 1985a; Shipp and Zeki, 1989a). There is also a known connection between some cells in layer 6 of the striate cortex and area MT (Fries et al., 1985; Shipp and Zeki, 1989a). Layer 4b also projects to specific sites in area V2 (Shipp and Zeki, 1985b), which in turn project to area MT (Shipp and Zeki, 1989b).

MT also receives a 'forward' input from area V3 (Ungerleider and Desimone, 1986a). It should be noted that MT feeds backwards to these same areas (Ungerleider and Desimone, 1986b; Shipp and Zeki, 1989a, 1989b). MT has 'intermediate' connections with areas V4, V3A and the parieto-occipital area (PO). There is also an input to MT from the superior colliculus that comes through the pulvinar nucleus of the thalamus (Beneveto and Standage, 1983). Indeed, the latter pathway may be of great importance as lesioning of the striate cortex by itself does not silence area MT (Rodman et al., 1989). However, combined lesions of striate cortex and the superior colliculus do (Rodman et al., 1990).

Area MT projects to several areas in the cortex. The most notable connections are the ones to the MST, the fundus superior temporal (FST) and the ventral intraparietal areas (VIP). It is believed that these areas may also be heavily involved in motion perception. There are also extensive feedback connections from these areas to area MT (Ungerleider and Desimone, 1986b). In turn area MST and FST make numerous connections in both the parietal and temporal cortex, and to the eye movement areas in the frontal cortex (Boussaoud et al., 1990).

This is only a brief survey of the pathway for visual motion perception. Many

connections and interrelations have not yet mentioned because of their complexity. Even given this brevity it is clear that MT plays a central role in such a motion pathway, that it has the potential to gather information about motion from many different sources, and its outpourings have consequences for many different visual functions.

5.2.2. Visual motion areas in the extrastriate cortex

Area MT/V5

It is now well established that monkey extrastriate cortex contains many different areas (for review, see Van Essen et al., 1992; Felleman and Van Essen, 1991). Of those 30 or more extrastriate areas, a small group in the caudal STS stands out, because their neurons share the property of direction selectivity, suggesting that these areas are involved in the analysis of retinal motion and in motion perception.

In the macaque monkey, area MT is located on the posterior bank and fundus of the STS. It is normally characterized anatomically by an area of dense myelination in the lower layers. Functionally, it contains a high concentration of neurons which are selective for the speed and the direction of stimulus motion (Zeki, 1974, 1978; Baker et al., 1981; Maunsell and Van Essen, 1983; Albright, 1984 Felleman and Kaas, 1984; Wurtz et al., 1990). MT is one of the few cortical areas that have been recognized across all primate species including humans (e.g. Van Essen, 1979; Bixby et al., 1980; Krubitzer and Kaas, 1990; Tootell et al., 1985, 1995).

Functional organizations of area MT/V5

The primate visual system incorporates a highly specialized subsystem for the

analysis of motion in the visual field. A key element of this subsystem is the MT. Area MT subdivides into a set of functionally distinct cortical areas. It contains a well-organized retinotopic map (Allman and Kaas, 1976; Sereno et al., 1994; Shmuel et al., 1996), and these highly specific patterns of connections reflect clear constraints on the types of relationships between different visual field locations that may be processed by MT neurons.

Area MT also contains a complicated compartmental architecture. In owl monkey MT, neurons sensitive to global and local motion are segregated in a band/interband architecture (Born and Tootell, 1992). Within each compartment, neurons showing preference to a particular line orientation are clustered in a columnar fashion (Malonek et al., 1994). A further subdivision of these orientation (or axis of motion) columns into opposing directionality columns has been proposed based on single-neuron studies in the macaque (Albright et al., 1984) and optical imaging studies in owl monkeys (Malonek et al., 1994).

In addition to MT's well known role in motion perception, it also plays an important role in stereoscopic depth perception. Experimental evidence from neurophysiological recordings in the MT area of the macaque monkey suggests that motion-selective cells can use disparity information to separate motion signals that originate from different depths. Recording extracellularly from MT neurons, DeAngelis and Newsome (1999) reported MT contains an abundance of disparity-sensitive neurons. In MT, neurons are clustered according to their disparity selectivity. Across the surface of MT, disparity-selective neurons are found in discrete patches that are separated by regions of MT that exhibit poor disparity tuning. Within disparity-selective patches of MT, they typically observe a smooth progression of preferred disparities (e.g., near to far) as the electrode travels parallel

to the cortical surface. In electrode penetrations to the cortical surface, on the other hand, MT neurons generally have a similar disparity tuning, with little variation from one recording site to the next. Thus disparity-tuned neurons are organized into cortical columns by preferred disparity, and preferred disparity is mapped systematically within larger, disparity-tuned patches of MT.

The human homologue of MT/V5

In human functional imaging, motion-related areas are generally identified by a comparison of the activation patterns induced by a uniformly moving stimulus and a stationary stimulus. Using this approach, neuroimaging studies (Zeki et al., 1991; Watson et al., 1993; Dupont et al., 1994, 1997; McCarthy et al., 1995; Tootell et al., 1995; Barton et al., 1996) have revealed a ventrolateral motion area, located posterior to the junction of the ascending limb of the inferior temporal and lateral occipital sulci. This area is considered to be the homologue of monkey area MT/V5, because of its strong differential motion activation and intense myelin and cytochrome staining (Clarke and Miklossy, 1990; Tootell and Taylor, 1995).

Other visual motion areas

Direction selective neurons predominate not only in the MT (Dubner and Zeki 1971; Lagae et al., 1994; Maunsell and Van Essen, 1983) but also in the MST (Desimone and Ungerleider, 1986; Lagae et al., 1994), VIP (Colby et al., 1993), and PO (Galletti et al., 1991) visual areas. Recent work on the visual system of primates has delineated several cortical fields involved in the processing of visual motion. These cortical areas appeared to be connected anatomically in stages, which suggests that there is a hierarchy in the machinery for motion perception. The most

prominent pathway for motion analysis begins in area V1 and proceeds through the MT/V5 to the MST. A large number of studies have been devoted to substantiating and clarifying the role of area MT/V5 and that of its satellites, the dorsal and ventral parts of the MST visual area.

5.2.3. Visual stimuli

Two types of moving stimuli have been used in physiological studies: restricted stimuli such as moving bars or slits which move through the receptive field, and large stimuli such as gratings or random dot patterns which cover the receptive field at all times. In the latter case, the receptive filed is stimulated by the motion of the elements in the stimulus, whereas the edges of the stimulus remain stationary.

Complex patterns such as visual noise and random dot patterns have been widely used in psychophysical research as well as in single cell recording because they contain no features which can be tracked frame to frame, thus allowing the isolation of the motion system (Nakayama and Tyler, 1981). Three advantages of random dot patterns are that their movement is detected by motion sensitive and not by position sensitive mechanisms. Second, the motion strength can be controlled without changing the luminance, contrast, position and shape of the visual stimuli. Finally a random pattern allows direct comparison between fine discriminations in speed and direction which are the two basic motion parameters.

The question then arises as to what the stimulus should be done in the interval between the motion presentations. Generally, the same stimulus as that used for the motion presentation is present but stationary, but this need not be the case. The dots, when present between motion presentations, need not be stationary for MT/V5 neurons to respond to the motion onset. For example, MT/V5 neurons will also

respond to the transition from flickering to moving random dots and to the transition from incoherently to coherently moving dots. In the second study, we chose stationary dots, coherent motion and/or random motion alternately presented in the visual field with different speeds (see Methods of the second study for the details).

5.2.4. Coherent and random motions

Psychological models and physiological studies in the macaque monkey show that directionally selective cells in V5 respond optimally to unidirectional coherent motion. Whereas those of V1 respond to motion within their receptive fields, regardless of the motion in surrounding parts. In contrast, McKeefry et al. (1997) reported that human V1/V2, V3, and V5 are all activated by both types of motion stimuli: coherent and incoherent motions. Incoherent (random) motion, however, proved to be more effective than coherent motion in activating V1/V2 and V5.

5.2.5. Motion onset and offset

Some studies have examined the human ability to react as quickly as possible after an object (or texture) starts to move at a constant velocity in the observer's visual field (motion onset) (Mashhour, 1964; Ball and Sekuler, 1980; Tynan and Sekuler, 1982). It has been established that the reaction time to motion onset decreases with increasing velocity of the stimulus. There is another kind of change in the velocity of stimuli, such as sudden increases, decreases, or full stops. If the motion stimulus is no longer moving it is known as the motion offset.

Using the dot pattern moving with speeds from 0.5 to 16° s^{-1}, then measuring the reaction time, Hohnsbein J and Mateeff S (1992) concluded that both stimulus

conditions, "motion-on" and "motion-off", yielded RTs that decrease with increasing velocity. The speed of "motion-on" affected the latency more than that of "motion-off". Dimitrov, Gourevich and Mateeff (1990) found that an increase in velocity of a "motion-off" stimulus from 2.5 to 5° s^{-1} leads to a significant decrease in the RT to the offset.

5.3. Objective

The objective of the second study was to investigate the physiological significance of the random motion detection in the visual system by comparing the MEG responses to coherent and random motions.

5.4. Subjects and Methods

Five healthy right-handed colleagues (three men and two women, aged 25-39) participated in this study. All had normal or corrected to normal visual acuity.

We used a RDK for the visual stimuli. It consisted of bright square dots (0.2 × 0.2° visual angle, 224 cd m^{-2}) randomly plotted on a dark background (10 × 10°, 4.3 cd m^{-2}). The density of the dots was determined to be 10% because neurons in monkey MT and V1 had maximum responses to the RDK at about this density in a previous study (Snowden et al., 1992). Two visual scenes (VS1 and VS2) created by RDK were alternately presented to the left visual field of the subject at randomly varied presentation times (2 to 3 s at steps of 0.2 s) (Fig. 10). The speed of dot motion was selected from 0, 0.6, 9.6, and 25° s^{-1} for comparison with the results of a previous study (ffytche et al., 1995). We used two types of dot motions, referred to as coherent (C) and random (R) motion in this study. For coherent motion, dots in each RDK frame were re-plotted with a fixed spatial offset in the same direction, so that all the

dots appeared to move in one direction at the same speed. Random dot motion was created by re-plotting each dot on a location, the direction of which was randomly chosen for each dot but which had the same spatial offset, so that the dots appeared to move at the same speed but did not evoke specific direction of motion globally. This also has been called "random-walk" (Scase et al., 1996). The direction of the coherent motion used was from left to right (towards the fixation point of the observer). Stimulus with a dot speed of 0 is referred to as S (Stationary). Speeds used in stimulus conditions C and R are indicated in the parentheses; e.g., C(0.6) indicates that the stimulus is coherent motion with a speed of 0.6° s^{-1}. Stimuli were generated by a VSG2/3 graphics board and projected on a screen inside the room by a video projector at the frame refresh rate of 75 Hz.

We recorded the magnetic responses from the right occipito-parieto-temporal region of the subject's brain to stimuli presented on the left visual field, using a 37-channel neuromagnetometer (Magnes, BTi) as in the first study (Fig. 11). Each subject lay on his/her right side on a bed in a dark magnetically shielded room (4.1 lux) and was instructed to gaze at the fixation point (red laser spot 0.2° in diameter) on the screen, which was offset 1.0° from the middle point of the right edge of the stimulus frame. The viewing distance was 150 cm. Because the visual stimulus consisted of the alternate presentation of VS1 and VS2, it caused two events in one MEG acquisition; stimulus change from VS1 to VS2 and from VS2 to VS1. MEG data of 50 ms before and 700 ms after each event were amplified in the frequency range from 0.1 to 800 Hz and digitized at a sampling rate of 2083.3 Hz until 125 epochs for each event were obtained. The data then were bandpass filtered at 1.0 to 80 Hz for further analysis. The DC level offset for each channel of MEG data was corrected to the mean value of the 50 ms data before the event. In order to reject artifacts related

to eye movements, EOG was recorded simultaneously. In the off-line averaging of the MEG and EOG data, MEG responses that drifted more than ± 3pT and EOGs that drifted more than $\pm 20\,\mu$V were discarded; therefore, from 100 to 120 magnetic responses were averaged for each event.

The peak latency and amplitude of the first component of the magnetic response were measured as RMS values across the 37 channels of averaged MEG data. The first component of the response was determined to be the first RMS deflection, the amplitude of which was more than 40 fT (twice of the background noise level). Responses whose RMS amplitudes were less than 40 fT were not analyzed. We used the single ECD model to estimate the location of the cortical activities and the strength of the current (dipole moment) that produced the magnetic fields. Criteria for the application of the model were that the estimated location of the ECD must be stable for at least 10 ms around the peak, and the correlation must be more than 0.95. The location then was superimposed on the MRI for each subject for the anatomical investigation. A three dimensional brain image for each subject was produced by the workstation (Indigo II, Silicon Graphics) with the aid of AVS (Advanced Visual Systems).

This experiment consisted of two sessions (see Fig. 10) with 30 stimulus conditions for each subject. In the first, magnetic responses to simple onset and offset of motions were investigated for different speeds and motion types. Responses to the onset and offset of coherent motion were evoked by the stimulus change between S (VS1) and C(VS2) at three different speeds of C. Similarly, onset and offset responses to random motion were evoked by the stimulus change between S and R. Each subject therefore needed six MEG acquisitions to obtain 12 magnetic responses for this session.

In the second session, whether the responses to motion type changes (from C to R or vise versa) differ from the responses to the simple onset or offset of both motions was investigated. If coherent motion is the "signal" and random motion is the "noise" in the visual motion detection system (Baker et al., 1991; Croner and Albright, 1999; Scase et al., 1996), the response to motion change from R to C would be similar to the response to the onset of coherent motion and the response to change from C to R would be similar to that to the offset of coherent motion. Two types of motion (R as VS1 and C as VS2) at three different speeds for each type were used to evoke magnetic responses. Therefore, nine (3 × 3) MEG acquisitions giving 18 magnetic responses, were made for each subject. The actual order of the stimulus conditions used for each subject was randomized for all 15 acquisitions in both sessions.

An ANOVA (General linear model in SYSTAT 7.0, SPSS Inc.) and the Wilcoxon test were used for the statistical evaluation of the effect of speed and the type of dot motion on the peak latency, amplitude, and current strength of the magnetic response. P values less than 0.05 were considered significant in all the analyses.

5.5. Results

All the subjects had good MEG responses to the visual stimuli under all the stimulus conditions used, but two of the total 150 responses were discarded because of low amplitude (less than 40 fT). The magnetic responses were composed of one to four components, depending on the subject and stimulus condition. We concentrated only on the first components because they had relatively large amplitudes and were easily distinguished.

5.5.1. Latency change in response to onset and offset of motion

Fig. 12 shows the waveforms of the magnetic responses and the RMS time courses to both onset and offset of coherent dot motion from a single subject (S10). As indicated, the peak latency of the first component was somewhat long at the lowest speed (0.6° s^{-1}) for coherent motion onset. This tendency is shown more clearly in the latency change of offset responses. Waveforms of the responses and their RMS to the onset and offset of random motion for the same subject are shown in Fig. 13. These were essentially the same as those for the coherent motion in Fig. 12. Latency changes in the first component of the offset responses also were the same as those for coherent motion offset responses, but the response latencies to random motion onset did not change with the speed.

Fig. 14 shows the peak latency changes in the first components of the onset and offset responses to both motion types for all subjects. Effects of subject and motion speed on the response latencies were assessed by a two-factor ANOVA. Speed had significant effect ($P<0.05$) on the latencies in the responses to the onset of coherent motion and to the offset of both coherent and random motions as indicated. Under these stimulus conditions, pairwise comparison using the Bonferroni adjustment indicated that the latencies for the speed of 0.6° s^{-1} were significantly longer than those for the other speeds, but there was no difference in the latencies of the speeds of 9.6 and 25° s^{-1}. In the comparison of the onset and offset response latencies for each motion type, a significant difference ($P<0.05$, paired t-test with Bonferroni adjustment) was found in the latencies for the speeds of 9.6 and 25° s^{-1}, but there was no difference in the offset response latencies of the coherent and random motions.

5.5.2. Latency change in response to motion type change

Figs. 15 and 16 show the waveforms of the magnetic responses and the time courses of the RMS values for responses to motion type changes in the second session. The peak latencies of the first components for the lowest speed (0.6° s^{-1}) of the preceding motion are longer than the others, but the speed of the subsequent motion did not affect the latencies in both motion type changes.

This tendency was found for all the subjects (Fig. 17). A significant effect ($P<0.001$) of preceding motion on latency was found by a three-factor ANOVA (subjects, preceding and subsequent motion speeds). Because there was no significant change in the latencies with the subsequent motion speed, the latencies for the responses to the motion type changes were averaged across the data for the same speed of preceding motion and compared in pairs with the latency changes for responses to the offset of motions done in the first session to check the possibility whether the subsequent motion speed affect the latency. Fig. 18 shows the mean (± S.D.) values of all the subjects data for four stimulus conditions (offset of coherent and random motions, motion type changes from random to coherent or vise versa) with three speeds of preceding motions. There was no significant difference in the latencies among the stimulus conditions for each speed ($P>0.05$, two-factors ANOVA) but the peak latencies for the lowest speed (0.6° s^{-1}) of the preceding motion in all the four stimulus conditions are longer than the others.

5.5.3. RMS amplitude and ECD moment of the magnetic response

Figs. 19 and 20 show the mean (±S.D.) for each subject for the peak RMS amplitudes for the first components and their ECD moments across the stimulus conditions used in the first and second sessions. In both sessions, there were no

statistically significant differences for either value under the stimulus conditions ($P>0.05$, two-factors ANOVA for the subjects and the stimulus conditions).

Because the response latencies to the motion type change were the same as those for the motion offset with the corresponding speed as shown above, the amplitudes and the ECD moments of the responses to the motion type changes were compared with those for the motion offset. All nine data in motion type change and three data in motion offset for each subject and motion type were averaged for this comparison, because there was no significant effect of speed on both amplitudes and ECD moments. As shown in Fig. 21, there was no significant difference in both values between each stimulus conditions.

5.5.4. Estimated origins of the magnetic responses

Totally, 30 magnetic responses were collected for each subject in the experimental sessions. Origins of 30, 16, 18, 20 and 29 responses were successfully estimated using the single ECD model for the subjects respectively of S10, S19, S29, S40, and S52. All the data are plotted in the individual graphs in Fig. 23. The mean location and mean + 2 S.D. of the distance from the mean location to the estimated locations also are shown on each graph. The estimated regions, overlaying on the three dimensional MRIs, are shown in Fig. 24.

For each subject, the mean coordinate of the estimated origin corresponded to the presumptive human MT/V5, reported in the previous PET (Watson et al., 1993) and fMRI studies (Tootell et al., 1995), but whether the area has the same physiological properties as monkey MT/V5 is controversial. A recent human PET study (Cornette et al., 1998) did not find involvement of MT/V5 in the detection of motion onset. A plausible explanation for this discrepancy is that transient neuronal

responses in human MT/V5 do not cause sufficient metabolic changes to be detected by PET.

5.5.5. Further analysis of the responses

The latency measurements showed that the preceding motion speed only affected the peak latency of the response to motion type change. A similar tendency was seen for the responses to onset and offset of motions (see Fig. 14) because the speed of preceding motion for onset is zero. To check this tendency, we plotted all the latency data for all the subjects according to preceding motion speed, as shown in Fig. 25. The data apparently could be divided into two groups; the slow response group for data at slow preceding motion speeds (0 and 0.6° s^{-1}), and the fast response group for data at fast preceding speeds (9.6 and 25° s^{-1}). Table 3 shows the stimulus conditions for these two groups.

This classification is supported by the estimated origins and the amplitude measurements. Fig. 26 shows differences in the distribution of the estimated dipole locations of the two groups. For all the subjects, the locations of the fast group responses were distributed medially (1.7 cm median across the mean values for all the subjects' data, $P<0.05$ by the Wilcoxon test) in contrast to the locations for the slow group. This is clearly shown in the graph of S10 whose data had smallest area of distribution, probably because of smaller measurement error. Mean RMS values of the slow response group for each subject were significantly larger than those of the fast response group, whereas the mean values of the dipole moment were not significant (see Table 4). The findings agree with the results of the estimated origins. This is because the RMS value (global strength of the magnetic field) for a response with an origin of longer distance (medial) from the MEG sensors (fast response

group) should be smaller than that for a response with an origin of shorter distance (slow response group) from the sensors, if the current strength of the dipole (moment) is the same for both groups.

Differences in the response properties of the subgroups in each response group was further investigated using the mean value across each subject's data in each subgroup. The results are shown in Table 4. In the slow response group, the estimated origins of the onset responses to coherent motion are located lateral (median: 0.7 cm, $P<0.05$ by the Wilcoxon test) to those for the onset responses to random motion, and the ECD moments of the former are smaller than those of the latter. Responses to the type change from random to coherent motion were estimated to originate from the region lateral (median: 1.1 cm, $P<0.05$ by the Wilcoxon test) to the locations for the responses to change from coherent to random motion. There was no difference in the offset response properties of the coherent and random motions in the slow response group. In the fast response group, offset responses had estimated locations anterior (median: 1.3 cm, $P<0.05$ by the Wilcoxon test) to those for the motion type changes and larger ECD moments than the latter. Other possible comparisons of the subgroups could not be done because of the small amount of data available. Fig. 27 shows a schematic illustration of the ECD location of each subgroup found in this study.

Two distinct distributions of the latency data may be related to the difference in the stimulus conditions between the two response groups instead of the preceding motion speeds or may be because we analyzed not only the first component (1M) but also the second component (2M) in the magnetic responses, if we hypothesize that 1M is very small in the conditions with the preceding motion speed of $0.6° s^{-1}$. We examined these possibilities with two subjects (S10 and S52). The latency changes of

the responses to the onset and offset of both coherent and random motions were measured with three speeds between 0.6 and 9.6° s^{-1} (1.2, 2.4, 4.8° s^{-1}). Fig. 28 shows the results for S52 who had the larger difference (150 ms) in the latency between two groups. As shown, the offset response latencies for both motions were inversely related to the speed of preceding motion with different response properties. That is, the offset response was less sensitive to the slow speed of random motion and the hypothesis that we analyzed two components was negated. In contrast, the onset latencies for both motions were not affected by the preceding motion speeds. The same tendency also was found for S10.

5.6. Discussion

Measurement of the magnetic response properties to various stimulus conditions for the two motions showed that (1) Both the onset and offset of random motion evoked magnetic responses similar to those for coherent motion in terms of amplitude and the estimated current strength of the dipoles. (2) Onset response to coherent motion at a speed of 0.6° s^{-1} had a longer latency than at other speeds; whereas, there was no latency change in the onset response to random motion. (3) Latencies of the offset responses to both motions at speeds of 9.6 and 25° s^{-1} were significantly shorter than were onset response latencies at those speeds. (4) Latencies of the responses to the motion type changes depended only on the speed of the preceding motions. (5) Responses could be divided into two groups based on the preceding motion speed. The slow response group at the preceding motion speeds of 0 or 0.6° s^{-1} had a slower (about 100 ms) response latency and more laterally (median 1.7 cm) located estimated origins than the fast response group at the preceding motion speeds of 9.6 and 25 ° s^{-1}. (6) In the slow response group, onset responses to

coherent motion had more laterally (median: 0.7 cm) located origins than the onset responses to random motion. Origins of the responses to change from random to coherent motion were estimated to be 1.1 cm lateral to those for change from coherent to random motion. (7) In the fast response group, origins of the responses to the offset motions were 1.3 cm anterior to those for the motion type changes. These findings indicate that coherent and random motions are processed in the adjacent cortical regions and the visual system has different subsystems for the detection of these motions.

5.6.1. Difference in response properties to both motions

Our latency change findings for onset responses to coherent motion correspond to those of a previous monkey experiment (Kawano et al. 1994). They found that the response latencies of monkey MST neurons to the visual motion similar to what we used were inversely related to speed in the range of 10 and 160° s^{-1}. Lagae et al. (1994) reported a similar tendency in the responses of monkey MT neurons but no statistical significance was given. The fact that the onset response latencies to coherent motion at speeds of 9.6 and 25° s^{-1} were shorter than for those at a speed of 0.6° s^{-1} may be explained by the existence of different neural pathways, as suggested by results of a previous MEG study (ffytche et al., 1995); i.e., the information that causes the longer latency response reaches the extrastriate cortex through V1 whereas the information for the shorter latency response reaches it via a shorter neural pathway. Unlike the onset response to coherent motion, the response latency to random motion did not change with the speed. This may not simply indicate that the extrastriate cortex is not sensitive to a speed of random motion, because the speed of the preceding random motion also affected the response latency to the offset

and motion type change (see Figs. 14 and 17).

Other response properties found to differ for coherent and random motions are the estimated origins and the ECD moments. Because ECD moment is considered to be related to neural activities (Hari and Lounasmaa, 1989; Hamalainen et al., 1993), the finding that the ECD moments for the random motion response were higher than for the coherent motion response (see Table 4) corresponds to results of a previous PET study (McKeefry et al., 1997) which showed that V1/V2 and V5 had a higher increase in blood flow in response to random motion than to coherent motion. The difference in the estimated response origins may not merely indicate the presence of the spatially segregated neural groups that process two motions, it also may be related to a difference in the distribution of neurons within the same region that are involved in the detection of the two motions. This is because the location estimated by the ECD model is considered to show the center of the current vectors created by many neural activities (Hamalainen et al., 1993), which may be the reason why we did not find a difference in the origins of the offset responses of the two motions. In any case, these facts indicate that response to the random motion is not merely due to the nonspecific excitation of the coherent motion detection system, although many direction selective neurons in monkey MT and even some neurons in the dorsomedial part of the medial superior temporal area (MSTd) respond to the random motion (Britten et al.,1993; Duffy and Wurtz, 1991).

This is supported further by the results of the latency change of the responses to motion type changes in the second session. Because the latency of the response from the extrastriate cortex was related to the speed of the preceding motion, neural activity related to the speed of random motion, as well as coherent motion, should exist in that cortical region. The fact that the latencies were related only to the speed

of the preceding motion does not simply indicate that the responses to motion changes were only related to the offset of the preceding motion, because the estimated origins of these responses differed from those for the offset responses in the fast response group (Fig. 27). In the slow response group, the response to motion changes for a preceding speed of 0.6° s^{-1} may be related to the onset response at the same speed, because the estimated origin of change from coherent to random motion is located anterior to that for change from random to coherent motion as is the estimated origin of the response to random motion onset at a speed of 0.6° s^{-1} (see Fig. 27). The results raise the possibility that the segregated subsystem for local motion processing found in the monkey brain (Born and Tootell, 1992) also exists in human and is related to the process of random motion, because the receptive fields of the neurons in the global motion detection system would be too wide to detect the speed of random motion.

What the neural process that is related to response latency changes with preceding motion speeds is not known. Amplitude of the early phasic response of the monkey MST neurons have been reported to be related to the response of preceding motion stimuli (Duffy and Wurtz, 1997), but they did not find response latency change. A few centimeters' difference in the origin of the response may not be sufficient to explain the 100 ms latency difference. One possibility is that offset of the preceding motion elevates the membrane potentials of the neurons involved in the direction of subsequent motion by the mechanism of disinhibition, resulting in the increase of neural responsibility.

We have to clearly show the reason why we only recorded the onset and offset responses, not the continuous activities (tonic responses) from the extrastriate cortex. In animal experiments, single neuronal recordings are usually done during

the steady stimulus conditions. They do not take so much care about the neural responses of beginning and ending of stimulus, which correspond to the neural responses to onset and offset of the stimulus. Such tonic responses between on and off of the neurons are considered to be related to the perception of presence of the stimulus. Our MEG measurement could not record brain activities related to these neural activities, probably because such neural activities are not synchronized enough to produce massive current to evoke measurable magnetic responses.

5.6.2. Possible role of random motion detection

Many MT neurons respond to dynamic masking noise dots (Britten et al., 1993), a visual stimulus similar to the random motion used in our study. This is consistent with the finding that MT neurons maintain spontaneous activities even when motion with anti-preferred direction is presented (Snowden et al., 1991). This response property does not seem to be necessary for the detection of motion; rather it would worsen the speed and direction tuning of the neurons, because suppression in the anti-preferred direction is a key mechanism of such tunings (Mikami et al., 1986). A recently presented model of visual motion detection in MT does not have this property, although it successfully simulated many cardinal features of MT neurons (Simoncelli and Heeger, 1998). This probably is not a "minor" discrepancy which could be compromised by adjusting the parameters in the model. We consider that this is evidence that MT has a function which can not be simulated by the model; i.e., the detection of random motion.

The existence of a neural mechanism to detect random motion would itself enhance the detectability of the coherent dot motion from the "noisy" background of randomly moving dots. This is because the contrast between the images of coherent

and random motion will increase if random dot motion in an entire visual scene is perceived as a homogeneous background of random motion. This speculation is supported by investigative findings for a patient who had the bilateral extrastriate damage (Baker, Jr. et al., 1991) that were based on a visual stimulus similar to ours. The patient had great difficulty in discriminating the direction of coherent dot motion when random dot motion was superimposed on the screen as noise. Although the patient could perfectly detect the direction of coherent motion without noise, this can not be attributed merely to a local motion detection mechanism which might be preserved with the intact V1. This is because the patient's direction discrimination was disturbed by stationary dots as strongly as by randomly moving dots mixed in the screen. We consider that the patient's visual system preserved the ability to integrate coherent motion but that it lost the ability to contrast coherent motion to random motion background.

5. General discussion and conclusions

In summary, in the first study continuous visual stimulation enhanced the middle-latency components of SEFs (at 35-60 msec in latency) but did not affect the short-latency components in the contralateral hemisphere. Auditory stimulation did not cause any change of waveforms. In contrast, the middle-latency component (70-100 msec in latency) recorded in the hemisphere ipsilateral to the stimulation disappeared or was markedly reduced in amplitude with either visual or auditory stimulation. Polymodal neurons in areas 5 and/or 7 and in the MST/STS may cause this particular phenomenon, but a change of attention may also be one of the causes.

In the second study, coherent and random onset and offset evoked magnetic responses from the human extrastriate cortex with the latency of the first component being 154-255 ms, depending on the speed of the preceding motion, except in the case of random motion onset. The ECD location data revealed that besides the well-known organizations of neurons in the extrastriate cortex, there may be an another organization, that is the human visual system has a subsystem for the process of random motion different from that for coherent motion. We consider that the presence of the subsystem to detect random motion increases the detectability of coherent motion in the visual scene of random motion.

In conclusion, using MEG we could assess the temporal and the spatial properties of the magnetic responses of the human cerebral cortex to multi-modal as well as uni-modal stimulation. With high spatial and temporal resolution, MEG seemed to be the best method available to investigate the complicated neural process in restricted areas.

7. Acknowledgments

My special gratitude is to Professor R. Kakigi as the supervisor for the studies in this Doctor thesis as well as for his initial encouragement and continued support and advice. He is one of the pioneers to do MEG. During the years of staying in Japan I had the pleasure of being his student.

I am indebted to Associate Professor Y. Kaneoke as the supervisor for the second study in this Doctor thesis. He is the one who initiated me into the field of visual evoked magnetic fields.

I am very grateful to Professor H. Komatsu, Dr. Hanazawa, Dr. M. Hoshiyama-(NIPS), Dr. A. Iriki, Department of Physiology, Toho University School of Medicine, for their valuable comments and suggestions.

My special thanks are to Dr. S. Koyama, Dr. H. Yamasaki, Miss. A. Gunji, Dr. S. Watanabe, Mr. T. Okusa, Dr. K. Maeda, Mr. T. Naito, Miss. E. Matsumoto, Mr. O. Nagata, Mr. Y. Takeshima for their technical help.

Little would have been accomplished without the invaluable secretarial help of Mrs. Y. Hyodo, Mrs. A. Fukuda and Miss. Y. Nonaka.

The invaluable assistance of Mr. M. Asai, Mr. Y. Hirooka and Ms. N. Sawada-the persons in charge of Student Affairs, Okazaki National Research Institutes is specially acknowledged for their attending the busy works to help students.

Finally, I extend my most sincere thanks to the Department of Integrative Physiology, National Institute for Physiological Sciences, Okazaki National Research Institutes, Graduate University for Advanced Studies, Ministry of Education, Science, Sports and Culture in Japan and their staff for their helps during my stay in Japan.

8. References

Abbruzzese G, Ratto S, Favale E, Abbruzzese M (1981) Proprioceptive modulation of somatosensory evoked potentials during active or passive finger movements in man. J. Neurol. Neurosurg. Psychiatry **44**: 942-949.

Albright TD (1984) Direction and orientation selectivity of neurons in visual area MT of the macaque. J. Neurophysiol. **52**: 1106-1130.

Albright TD, Desimone R, Gross CG (1984) Columnar organization of directionally selective cells in visual area MT of the macaque. J. Neurophysiol. **51**: 16-31.

Allison T, McCarthy G, Wood CC, Darcey TM, Spencer DD, Williamson PD (1989a) Human cortical potentials evoked by stimulation of the median nerve. I. Cytoarchitectonic areas generating short-latency activity. J. Neurophysiol. **62**:694-710.

Allison T, McCarthy G, Wood CC, Williamson PD, Spencer DD (1989b) Human cortical potentials evoked by stimulation of the median nerve. II. Cytoarchitectonic areas generating long-latency activity. J. Neurophysiol. **62**: 711-722.

Allman JM, Kaas JH (1976) Representation of the visual field on the medical wall of occipital-parietal cortex in the owl monkey. Science **191**: 572-575.

Baker CL Jr, Hess RF, Zihl J (1991) Residual motion perception in a "motion-blind" patient, assessed with limited-lifetime random dot stimuli. J. Neurosci. **11**: 454-461.

Baker JF, Petersen SE, Newsome WT, Allman JM (1981) Visual response properties of neurons in four extrastriate visual areas of the owl monkey (Aotus trivirgatus): a quantitative comparison of medial, dorsomedial, dorsolateral, and

middle temporal areas. J. Neurophysiol. **45**: 397-416.

Ball K, Sekuler R (1980) Models of stimulus uncertainty in motion perception. Psychol. Rev. **87**: 435-469.

Barton JJS, Simpson T, Kiriakopoulos E, Stewart C, Crawley A, Guthrie, et al. (1996) Functional MRI of lateral occipitotemporal cortex during pursuit and motion perception. Ann. Neurol. **40**: 387-398.

Baumgartner C, Sutherling WW, Di S, Barth DS (1991) Spatiotemporal modeling of cerebral evoked magnetic fields to median nerve stimulation. Electroenceph. clin. Neurophysiol. **79**: 27-35.

Benevento LA, Standage GP (1983) The organization of projections of the retinorecipient and nonretinorecipient nuclei of the pretectal complex and layers of the superior colliculus to the lateral pulvinar and medial pulvinar in the macaque monkey. J. Comp. Neurol. **217**: 307-336.

Bixby JL, Maunsell JH, Van Essen DC (1980) Effects of motor unit size on innervation patterns in neonatal mammals. Exp. Neurol. **70**: 516-524.

Born RT, Tootell RB (1992) Segregation of global and local motion processing in primate middle temporal visual area. Nature **357**: 497-499.

Boussaoud D, Ungerleider LG, Desimone R (1990) Pathways for motion analysis: cortical connections of the medial superior temporal and fundus of the superior temporal visual areas in the macaque. J. Comp. Neurol. **296**: 462-495.

Britten KH, Shadlen MN, Newsome WT, Movshon JA (1993) Responses of neurons in macaque MT to stochastic motion signals. Vis. Neurosci. **10**: 1157-1169.

Bruce C, Desimone R, Gross CG (1981) Visual properties of neurons in a polysensory area in superior temporal sulcus of the macaque. J. Neurophysiol. **46**: 369-384.

Cheron G, Borenstein S (1991) Gating of the early components of the frontal and parietal somatosensory evoked potentials in different sensory-motor interference modalities. Electroencephalogr. clin. Neurophysiol. **80**: 522-530.

Clarke S, Miklossy J (1990) Occipital cortex in man: organization of callosal connections, related myelo- and cytoarchitecture, and putative boundaries of functional visual areas. J. Comp. Neurol. **298**: 188-214.

Cohen LG, Starr A (1987) Localization, timing and specificity of gating of somatosensory evoked potentials during active movement in man. Brain **110** (Pt 2): 451-467.

Colby CL, Duhamel JR, Goldberg ME (1993) Ventral intraparietal area of the macaque: anatomic location and visual response properties. J. Neurophysiol. **69**: 902-914.

Cornette L, Dupont P, Spileers W, Sunaert S, Michiels J, Van Hecke P, Mortelmans L, Orban GA (1998) Human cerebral activity evoked by motion reversal and motion onset. A PET study. Brain **121** (Pt 1): 143-157.

Croner LJ, Albright TD (1999) Segmentation by color influences responses of motion-sensitive neurons in the cortical middle temporal visual area. J. Neurosci. **19**: 3935-3951.

DeAngelis GC, Newsome WT (1999) Organization of disparity-selective neurons in macaque area MT. J. Neurosci. **19**: 1398-1415.

Desimone R, Ungerleider LG (1986) Multiple visual areas in the caudal superior temporal sulcus of the macaque. J. Comp. Neurol. **248**: 164-189.

Desmedt JE, Nguyen TH, Bourguet M (1983) The cognitive P40, N60 and P100 components of somatosensory evoked potentials and the earliest electrical signs of sensory processing in man. Electroenceph. clin. Neurophysiol. **56**: 272-282.

Dimitrov G, Gourevich A, Mateeff S (1990) Reaction time to motion offset of visual stimuli. Comptes rendus de l'Academie bulgare des Sciences **43**: 83-86.

Dubner R, Zeki SM (1971) Response properties and receptive fields of cells in an anatomically defined region of the superior temporal sulcus in the monkey. Brain Res. **35**: 528-532.

Duffy CJ, Wurtz RH (1991) Sensitivity of MST neurons to optic flow stimuli. I. A continuum of response selectivity to large-field stimuli. J. Neurophysiol. **65**: 1329-1345.

Duffy CJ, Wurtz RH (1997) Multiple temporal components of optic flow responses in MST neurons. Exp. Brain Res. **114**: 472-482.

Dupont P, De Bruyn B, Vandenberghe R, Rosier AM, Michiels J, Marchal G, Mortelmans L, Orban GA (1997) The kinetic occipital region in human visual cortex. Cereb. Cortex **7**: 283-292.

Dupont P, Orban GA, De Bruyn B, Verbruggen A, Mortelmans L (1994) Many areas in the human brain respond to visual motion. J. Neurophysiol. **72**: 1420-1424.

Felleman DJ, Kaas JH (1984) Receptive-field properties of neurons in middle temporal visual area (MT) of owl monkeys. J. Neurophysiol. **52**: 488-513.

Felleman DJ, Van Essen DC (1991) Distributed hierarchical processing in the primate cerebral cortex. Cereb. Cortex **1**: 1-47.

ffytche DH, Guy CN, Zeki S (1995) The parallel visual motion inputs into areas V1 and V5 of human cerebral cortex. Brain **118**: 1375-1394.

Fries W, Keizer K, Kuypers HG (1985) Large layer VI cells in macaque striate cortex (Meynert cells) project to both superior colliculus and prestriate visual area V5. Exp. Brain Res. **58**: 613-616.

Galletti C, Battaglini PP, Fattori P (1991) Functional properties of neurons in the anterior bank of the parieto-occipital sulcus of the macaque monkey. Eur. J. Neurosci. **3**: 452-461.

Hamalainen M, Hari R, IImoniemi RJ, Knuutila J, Lounasmaa OV (1993) Magnetoencephalography - theory, instrumentation, and applications to nonivasive studies of the working human brain. Rev. Mod. Phys. **65**: 413-497.

Hari R, Hamalainen H, Hamalainen M, Kekoni J, Sams M, Tiihonen J (1990) Separate finger representations at the human second somatosensory cortex. Neuroscience **37**: 245-249.

Hari R, Lounasmaa OV (1989) Recording and interpretation of cerebral magnetic fields. Science **244**: 432-436.

Hari R, Reinikainen K, Kaukoranta E, Hamalainen M, Ilmoniemi R, Penttinen A, Salminen J, Teszner D (1984) Somatosensory evoked cerebral magnetic fields from S1 and S2 in man. Electroencephalogr. clin. Neurophysiol. **57**: 254-263.

Hikosaka K, Iwai E, Saito H, Tanaka K (1988) Polysensory properties of neurons in the anterior bank of the caudal superior temporal sulcus of the macaque monkey. J. Neurophysiol. **60**: 1615-1637.

Hohnsbein J, Mateeff S (1992) The relation between the velocity of visual motion and the reaction time to motion onset and offset. Vision Res. **32**: 1789-1791.

Hubel DH, Wiesel TN (1972) Laminar and columnar distribution of geniculo-cortical fibers in the macaque monkey. J. Comp. Neurol. **146**: 421-450.

Huttunen J, Hari R, Leinonen L (1987) Cerebral magnetic responses to stimulation of ulnar and median nerves. Electroenceph. clin. Neurophysiol. **66**: 391-400.

Hyvarinen J (1981) Regional distribution of functions in parietal association area 7 of the monkey. Brain Res. **206**: 287-303.

Hyvarinen J, Poranen A (1974) Function of the parietal associative area 7 as revealed from cellular discharges in alert monkeys. Brain **97**: 673-692.

Jones EG, Powell TP (1970) An anatomical study of converging sensory pathways within the cerebral cortex of the monkey. Brain **93**: 793-820.

Jones SJ (1981) An "interference" approach to the study of somatosensory evoked potentials in man. Electroencephalogr. clin. Neurophysiol. **52**: 517-530.

Jones SJ, Power CN (1984) Scalp topography of human somatosensory evoked potentials: the effect of interfering tactile stimulation applied to the hand. Electroencephalogr. Clin. Neurophysiol. **58**: 25-36.

Kakigi R (1986) Ipsilateral and contralateral SEP components following median nerve stimulation: effects of interfering stimuli applied to the contralateral hand. Electroencephalogr. Clin. Neurophysiol. **64**: 246-259.

Kakigi R, Jones SJ (1985) Effects on median nerve SEPs of tactile stimulation applied to adjacent and remote areas of the body surface. Electroencephalogr. clin. Neurophysiol. **62**: 252-265.

Kakigi R, Jones SJ (1986) Influence of concurrent tactile stimulation on somatosensory evoked potentials following posterior tibial nerve stimulation in man. Electroencephalogr. clin. Neurophysiol. **65**: 118-129.

Kakigi R (1994) Somatosensory evoked magnetic fields following median nerve stimulation. Neurosci. Res. **20**: 165-174.

Kakigi R, Koyama S, Hoshiyama M, Watanabe S, Shimojo M, Kitamura Y (1995) Gating of somatosensory evoked responses during active finger movements: magnetoencephalographic studies. J. Neurol. Sci. **128**: 195-204.

Kakigi R, Koyama S, Hoshiyama M, Kitamura Y, Shimojo M, Watanabe S, Nakamura A (1996) Effects of tactile interference stimulation on somatosensory

evoked magnetic fields. NeuroReport **7**: 405-408.

Kakigi R, Shimojo M, Hoshiyama M, Koyama S, Watanabe S, Naka D, Suzuki H, Nakamura A (1997) Effects of movement and movement imagery on somatosensory evoked magnetic fields following posterior tibial nerve stimulation. Brain Res. Cogn. Brain Res. **5**: 241-253.

Kaneoke Y, Bundou M, Koyama S, Suzuki H, Kakigi R (1997) Human cortical area responding to stimuli in apparent motion. NeuroReport **8**: 677-682.

Kawano K, Shidara M, Watanabe Y, Yamane S (1994) Neural activity in cortical area MST of alert monkey during ocular following responses. J. Neurophysiol. **71**: 2305-2324.

Kazakov VN, Shevchenko NI, Krakhotkina ED (1981) Associative connections of the parietal cortex in cats. Neirofiziologiia **13**: 3-6.

Komatsu H (1993) Neural coding of color and form in the inferior temporal cortex of the monkey. Biomed. Res. **14**: 7-13.

Komatsu H, Murakami I, Kinoshita M (1996) Surface representation in the visual system. Brain Res. Cogn. Brain Res. **5**: 97-104.

Krubitzer LA, Kaas JH (1990) Cortical connections of MT in four species of primates: areal, modular, and retinotopic patterns. Vis. Neurosci. **5**: 165-204.

Lagae L, Maes H, Raiguel S, Xiao DK, Orban GA (1994) Responses of macaque STS neurons to optic flow components: a comparison of areas MT and MST. J. Neurophysiol. **71**: 1597-1626.

Lee RG, White DG (1974) Modification of the human somatosensory evoked response during voluntary movement. Electroencephalogr. clin. Neurophysiol. **36**: 53-62.

Leinonen L, Hyvarinen J, Nyman G, Linnankoski I (1979) I. Functional properties of neurons in lateral part of associative area 7 in awake monkeys. Exp. Brain Res.

34: 299-320.

Leinonen L, Nyman G (1979) II. Functional properties of cells in anterolateral part of area 7 associative face area of awake monkeys. Exp. Brain Res. **34**: 321-333.

Malonek D, Tootell RB, Grinvald A (1994) Optical imaging reveals the functional architecture of neurons processing shape and motion in owl monkey area MT. Proc. R. Soc. Lond. B. Biol Sci. **258**: 109-119.

Mashhour M (1964) Psychophysical relations in the perception of velocity. Stockholm: Almquist & Wiksell.

Maunsell JH, Van Essen DC (1983) Functional properties of neurons in middle temporal visual area of the macaque monkey. I. Selectivity for stimulus direction, speed, and orientation. J. Neurophysiol. **49**: 1127-1147.

McCarthy G, Spicer M, Adrignolo A, Luby M, Gore J, Allison T (1995) Brain activation associated with visual motion studied by functional magnetic resonance imaging in humans. Hum. Brain Mapp. **2**: 234-243.

McKeefry DJ, Watson JD, Frackowiak RS, Fong K, Zeki S (1997) The activity in human areas V1/V2, V3, and V5 during the perception of coherent and incoherent motion. Neuroimage **5**: 1-12.

Mikami A, Newsome WT, Wurtz RH (1986) Motion selectivity in macaque visual cortex. I. Mechanisms of direction and speed selectivity in extrastriate area MT. J. Neurophysiol. **55**: 1308-1327.

Morgan MJ, Ward R (1980) Conditions for motion flow in dynamic visual noise. Vision Res. **20**: 431-435.

Naka D, Kakigi R, Koyama S, Xiang J, Suzuki H (1998) Effects of tactile interference stimulation on somatosensory evoked magnetic fields following tibial nerve stimulation. Electroencephalogr. clin. Neurophysiol. **109**: 168-177.

Nakayama K, Tyler CW (1981) Psychophysical isolation of movement sensitivity by removal of familiar position cues. Vision Res. **21**: 427-433.

Narikashvili SP, Kadzhaia DV, Timchenko AS, Narikashvili MS (1977) Interaction between spindles evoked by electric stimulation of different regions of the cerebral cortex. Fiziol. Zh. SSSR **63**: 3-10.

Neal JW, Pearson RC, Powell TP (1987) The cortico-cortical connections of area 7b, PF, in the parietal lobe of the monkey. Brain Res. **419**: 341-346.

Neal JW, Pearson RC, Powell TP (1990) The ipsilateral cortico-cortical connections of area 7b, PF, in the parietal and temporal lobes of the monkey. Brain Res. **524**: 119-132.

Newsome WT, Pare EB (1988) A selective impairment of motion perception following lesions of the middle temporal visual area (MT). J. Neurosci. **8**: 2201-2211.

Newsome WT, Britten KH, Movshon JA (1989) Neuronal correlates of a perceptual decision. Nature **341**: 52-54.

Okada YC, Wu J, Kyuhou S (1997) Genesis of MEG signals in a mammalian CNS structure. Electroencephalogr. clin. Neurophysiol. **103**: 474-485.

Pandya DN, Seltzer B (1982) Association areas of the cerebral cortex. Trends in Neurosci. **5**: 386-390.

Pearson RC, Powell TP (1985) The projection of the primary somatic sensory cortex upon area 5 in the monkey. Brain Res. **356**: 89-107.

Rodman HR, Gross CG, Albright TD (1989) Afferent basis of visual response properties in area MT of the macaque. I. Effects of striate cortex removal. J. Neurosci. **9**: 2033-2050.

Rodman HR, Gross CG, Albright TD (1990) Afferent basis of visual response properties in area MT of the macaque. II. Effects of superior colliculus removal.

J. Neurosci. **10**: 1154-1164.

Rossini PM, Narici L, Romani GL, Peresson M, Torrioli G, Traversa R (1989) Simultaneous motor output and sensory input: cortical interference site resolved in humans via neuromagnetic measurements. Neurosci Lett. **96**: 300-305.

Salzman CD, Britten KH, Newsome WT (1990) Cortical microstimulation influences perceptual judgements of motion direction. Nature **346**: 174-177.

Sarvas J (1987) Basic mathematical and electromagnetic concepts of the biomagnetic inverse problem. Phys. Med. Biol. **32**: 11-22.

Scase MO, Braddick OJ, Raymond JE (1996) What is noise for the motion system? Vision Res. **36**: 2579-2586.

Sereno MI, McDonald CT, Allman JM (1994) Analysis of retinotopic maps in extrastriate cortex. Cereb. Cortex **4**: 601-620.

Shipp S, Zeki S (1985a) Segregated output to area V5 from layer 4B of macaque monkey striate cortex. J. Physiol. (Lond.), **369**, 32P.

Shipp S, Zeki S (1985b) Segregation of pathways leading from area V2 to areas V4 and V5 of macaque monkey visual cortex. Nature **315**: 322-325.

Shipp S, Zeki S (1989a) The organization of connections between areas V5 and V1 in macaque monkey visual cortex. Eur. J. Neurosci. **1**: 309-332.

Shipp S, Zeki S (1989b) The organization of connections between areas V5 and V2 in macaque monkey visual cortex. Eur. J. Neurosci. **1**: 333-354.

Shmuel A, Schirman TD, Harel M, Malonek D, Grinvald A, Malach R (1996) Optical cartography: simultaneous retinotopic and functional mapping of several areas in primate visual cortex using optical imaging. Soc. Neurosci. Abstr 22: 760.11 (Abstract).

Siegel RM, Andersen RA (1988) Perception of three-dimensional structure from motion in monkey and man. Nature **331**: 259-261.

Simoncelli EP, Heeger DJ (1998) A model of neuronal responses in visual area MT. Vision Res. **38**: 743-761.

Snowden RJ, Treue S, Erickson RG, Andersen RA (1991) The response of area MT and V1 neurons to transparent motion. J. Neurosci. **11**: 2768-2785.

Snowden RJ, Treue S, Andersen RA (1992) The response of neurons in areas V1 and MT of the alert rhesus monkey to moving random dot patterns. Exp. Brain Res. **88**: 389-400.

Tiihonen J, Hari R, Hamalainen M (1989) Early deflections of cerebral magnetic responses to median nerve stimulation. Electroenceph. clin. Neurophysiol. **74**: 290-296.

Tootell RB, Hamilton SL, Silverman MS (1985) Topography of cytochrome oxidase activity in owl monkey cortex. J. Neurosci. **5**: 2786-2800.

Tootell RB, Reppas JB, Kwong KK, Malach R, Born RT, Brady TJ, Rosen BR, Belliveau JW (1995) Functional analysis of human MT and related visual cortical areas using magnetic resonance imaging. J. Neurosci. **15**: 3215-3230.

Tootell RB, Taylor JB (1995) Anatomical evidence for MT and additional cortical visual areas in humans. Cereb. Cortex **5**: 39-55.

Touge T, Takeuchi H, Sasaki I, Deguchi K, Ichihara N (1997) Enhanced amplitude reduction of somatosensory evoked potentials by voluntary movement in the elderly. Electroencephalogr. clin. Neurophysiol. **104**: 108-114.

Tynan PD, Sekuler R (1982) Motion processing in peripheral vision: reaction time and perceived velocity. Vision Res. **22**: 61-68.

Ungerleider LG, Desimone R (1986a) Projections to the superior temporal sulcus from the central and peripheral field representations of V1 and V2. J. Comp. Neurol. **248**: 147-163.

Ungerleider LG, Desimone R (1986b) Cortical connections of visual area MT in the macaque. J. Comp. Neurol. **248**: 190-222.

Van Essen DC (1979) Visual areas of the mammalian cerebral cortex. Annu. Rev. Neurosci. **2**: 227-263.

Van Essen DC, Maunsell JH, Bixby JL (1981) The middle temporal visual area in the macaque: myeloarchitecture, connections, functional properties and topographic organization. J. Comp. Neurol. **199**: 293-326.

Van Essen DC, Anderson CH, Felleman DJ (1992) Information processing in the primate visual system: an integrated systems perspective. Science **255**: 419-423.

Watson JD, Myers R, Frackowiak RS, Hajnal JV, Woods RP, Mazziotta JC, Shipp S, Zeki S (1993) Area V5 of the human brain: evidence from a combined study using positron emission tomography and magnetic resonance imaging. Cereb. Cortex **3**: 79-94.

Williams DW, Sekuler R (1984) Coherent global motion percepts from stochastic local motions. Vision Res. **24**: 55-62.

Wood CC, Cohen D, Cuffin BN, Yarita M, Allison T (1985) Electrical sources in human somatosensory cortex: identification by combined magnetic and potential recordings. Science **227**: 1051-1053.

Wurtz RH, Yamasaki DS, Duffy CJ, Roy JP (1990) Functional specialization for visual motion processing in primate cerebral cortex. Cold Spring Harb. Symp. Quant. Biol. **55**: 717-727.

Xiang J, Hoshiyama M, Koyama S, Kaneoke Y, Suzuki H, Watanabe S, Naka D, Kakigi, R (1997) Somatosensory evoked magnetic fields following passive finger movement. Brain Res. Cogn. Brain Res. **6**: 73-82.

Zeki S, Watson JD, Lueck CJ, Friston KJ, Kennard C, Frackowiak RS (1991) A direct demonstration of functional specialization in human visual cortex. J. Neurosci. **11**: 641-649.

Zeki SM (1974) Functional organization of a visual area in the posterior bank of the superior temporal sulcus of the rhesus monkey. J. Physiol. (Lond.) **236**: 549-573.

Zeki SM (1978) Uniformity and diversity of structure and function in rhesus monkey prestriate visual cortex. J. Physiol. (Lond) **277**: 273-290.

9. Tables

Table 1: Amplitude and root mean square (RMS) in all five components in each multi-modal stimulus condition in 12 subjects expressed as percentage based on the values of the control waveform (100%).

Interference	Component	Amplitude	RMS
Cartoon	1M	97.3±7.4	97.5±13.3
	2M	104.6±12.1	102.5±9.9
	3M	110.6±12.3**	112.3±20.1*
	4M	109.8±9.1***	110.3±7.7***
	MI	61.0±27.5***	62.1±22.3***
Random dots	1M	96.0±8.8	99.3±13.3
	2M	100.6±9.6	100.5±9.1
	3M	111.6±16.6*	113.7±17.3**
	4M	102.7±11.4	103.3±17.3
	MI	87.9±57.0	85.9±55.2
Music	1M	95.4±8.6	95.9±13.0
	2M	99.4±8.0	98.9±10.0
	3M	105.6±15.0	108.6±15.8
	4M	103.2±13.2	100.8±10.7
	MI	66.3±28.7**	70.3±29.3*

Values are shown as mean±standard deviation. The number of subjects is 12 for 1M-4M and 7 for MI.

*** $P<0.01$, ** $P<0.02$, * $P<0.05$ by paired t-test between control and each multi-modal stimulus condition.

Table 2: The x, y and z coordinates (cm) of ECD of the five components recorded in control and each multi-modal stimulus condition.

	Component	x	y	z
Control	1M	2.7±1.0	-4.4±0.6	9.6±0.6
	2M	2.9±1.1	-4.2±0.8	9.6±0.9
	3M	2.7±1.0	-4.2±0.5	10.0±0.8
	4M	2.4±1.2	-4.0±1.1	9.8±0.8
	MI	2.3±0.8	4.8±0.4	6.4±0.4
Cartoon	1M	2.7±1.0	-4.4±0.5	9.7±0.7
	2M	2.7±1.0	-4.3±0.7	9.8±0.6
	3M	2.5±1.0*	-4.1±0.5	10.0±0.7
	4M	2.3±1.1	-4.1±0.7	9.8±1.0
	MI	2.1±0.8	4.7±0.3	6.2±0.5
Random dots	1M	2.7±1.1	-4.2±0.8	9.6±0.6
	2M	2.8±1.0	-4.4±0.7	9.8±0.6
	3M	2.6±1.0	-4.2±0.5	10.0±0.8
	4M	2.5±1.1	-4.1±0.9	9.7±0.9
	MI	2.3±0.9	5.0±0.5	6.5±0.4
Music	1M	2.8±1.0	-4.5±0.6	9.6±0.6
	2M	2.7±1.1	-4.2±0.9	9.6±0.7
	3M	2.5±1.1	-3.9±0.6	9.9±0.8
	4M	2.5±1.1	-4.0±0.9	9.8±1.0
	MI	2.6±0.7	5.0±0.7	6.2±0.6

The number of subjects is 12 for 1M-4M and 7 for MI.

* $P<0.01$ by paired t-test between the control and the cartoon session.

Table 3: Stimulus conditions for the two groups.

Slow responses			Fast responses		
Onset of motion					
S-C(0.6)	S-C(9.6)	S-C(25)			
S-R(0.6)	S-R(9.6)	S-R(25)			
Offset of motion at a slow preceding speed			Offset of motions at a high preceding speed		
C(0.6)-S			C(9.6)-S	C(25)-S	
R(0.6)-S			R(9.6)-S	R(25)-S	
Motion type changes at a slow preceding speed			Motion type changes at a high preceding speed		
C(0.6)-R(0.6)	C(0.6)-R(9.6)	C(0.6)-R(25)	C(9.6)-R(0.6)	C(9.6)-R(9.6)	C(9.6)-R(25)
R(0.6)-C(0.6)	R(0.6)-C(9.6)	R(0.6)-C(25)	C(25)-R(0.6)	C(25)-R(9.6)	C(25)-R(25)
			R(9.6)-C(0.6)	R(9.6)-C(9.6)	R(9.6)-C(25)
			R(25)-C(0.6)	R(25)-C(9.6)	R(25)-C(25)

Table 4: Comparison of response properties for four parameters.

	Latency (ms)	Dipole location (cm)			RMS (fT)	ECD Moment (nAm)
		X	Y	Z		
Slow response	255.1	-2.2	-3.6	6.4	73.6	22.1
Fast response	154.3*	-1.9	-1.9*	6.1	62.1*	31.4
Slow response group						
Onset (C)	268.8	-2.1	-4.3	6.4	66.3	18.7
Onset (R)	254.4	-2.1	-3.6*	6.4	89.2	25.5*
Offset (C)	262.6	-1.2	-3.9	6.1	64.5	20.7
Offset (R)	253.4	-2.1	-3.6	6.4	79.2	19.7
Change (R-C)	264.3	-2.2	-3.8	6.4	74.1	30.0
Change (C-R)	262.4	-2.2	-2.7*	6.3	71.8	30.0
Fast response group						
Offset (C)	175.2	-1.3	-3.2	6.2	68.6	41.6
Offset (R)	192.2	-0.8	-2.6	5.7	67.0	37.3
Change (R-C)	167.3	-2.4	-2.1	5.7	57.6	29.9
Change (C-R)	143.0	-2.1	-2.4	6.1	59.8	28.4
Offset	183.7	-1.0	-1.9	5.7	80.2	35.1
Change	155.1	-2.3*	-1.9	5.7	62.2	30.3*

Mean values across the data in each subgroup for each subject were compared by the Wilcoxon test. The median for each group is shown. Values that are significantly different ($P<0.05$) from the above values are indicated by the asterisks (*). C: response to coherent motion; R: response to random motion; C-R: response to change from coherent to random motion; R-C: response to change from random to coherent

motion. Note that a small Y value indicates a more medial and a larger X value does a more anterior region.

10. Figure legends

Figure 1: SEFs following the left median nerve stimulation recorded at the C4 (contralateral) and C3 (ipsilateral) positions in the control session in subject 6. All waveforms recorded at 37 channels were superimposed to indicate the nomenclature of each component. Four main components (1M, 2M, 3M and 4M) were identified in the contralateral hemisphere, and one middle-latency component (MI) was found in the ipsilateral hemisphere. M: Magnetic field.

Figure 2: The waveforms recorded at all 37 channels (left) and the isocontour map of the 1M component (right) in the control session in subject 6 at the latency of 17.3 ms indicated by the vertical line in the left figure (see also Fig. 1). The probe was centered on the C4 position (International 10-20 system). The outward flux is marked by solid lines in the contour plot, the inward flux is shown by dotted lines, and the thick line shows the zero point. The contour step was 10fT.

Figure 3: Averaged waveforms of the magnetic responses recorded at the C4 position (contralateral) in the control and each multi-modal stimulus condition in subject 11 (a) and subject 12 (b). (a) The middle-latency components (3M and 4M) were enhanced in the cartoon and dots sessions. (b) 3M and 4M were enhanced in the cartoon session, but no significant change was found in the dots and music sessions.

Figure 4: Amplitude and RMS changes of the 3M (upper) and 4M (lower) components in each session in 12 subjects. A significant enhancement of both amplitude and RMS of the 3M in the cartoon and dots sessions and of the 4M in the cartoon session was found by the paired t-test, as indicated by the P values.

Figure 5: Averaged waveforms of the magnetic responses recorded at the C3 position (ipsilateral) in the control and each multi-modal stimulus condition in subject 11 (a) and subject 12 (b). (a) The middle-latency component (MI) was markedly attenuated in all three multi-modal stimulus conditions. (b) MI was markedly attenuated in the cartoon and music sessions (especially in the cartoon session), but was not changed in the dots session.

Figure 6: The localization of ECDs of the 1M component recorded at the C4 position (contralateral) in the control and each multi-modal stimulus condition, overlapped on coronal views of MRI in subject 6. The ECDs are located on the hand area of S1 in the right hemisphere.

Figure 7: Localization of ECDs of the middle-latency (3M) component indicated by Figure 3 (b), which was enhanced in the cartoon session, recorded at the C4 position in subject 12. The ECDs were around the hand area of the S1 contralateral to the stimulated median nerve.

Figure 8: Localization of ECDs of the middle-latency (4M) component indicated by Figure 3 (b), which was enhanced in the cartoon session, recorded at the C4 position in subject 12. The ECDs were around the hand area of the S1 contralateral to the stimulated median nerve.

Figure 9: Localization of ECDs of the middle-latency (MI) component indicated by Figure 5 (b), which was markedly attenuated in the cartoon and music sessions (especially in the cartoon session), recorded at the C3 position in subject 12. The ECDs were located around the superior bank of the Sylvian fissure, i.e., the S2 in the left hemisphere.

Figure 10: Schematic illustration of the visual stimuli used in the two experimental sessions. They consisted of alternate presentation (2-3 s) of two different RDKs (VS1 and VS2). In the first session, two types of motions (coherent and random dot motions) were used for VS2, whereas VS1 was randomly plotted stationary dots. In this session, magnetic responses to both onset (change from VS1 to VS2) and offset (change from VS2 to VS1) of the two motions were investigated at three speeds (0.6, 9.6, and 25° s^{-1}). In the second session, magnetic responses to the change in motion type at three speeds were investigated. Randomly moving dots (VS1) at the speed of one of three then coherently moving dots (VS2) at a speed of three were alternately presented for 2 to 3 s.

Figure 11: The recording area with the sensor layout was shown on the right hemisphere. The center of the probe was placed around the O2, P4, T6 positions (according to the International 10-20 System). That is, we recorded the magnetic responses from the right occipito-parieto-temporal region of the subject's brain to stimuli presented on the left visual field.

Figure 12: Averaged waveforms of the magnetic responses and the time courses of the RMS values to the onset (S-C) and offset (C-S) of coherent motion for one subject (S10) are shown for each speed. Waveforms from the magnetic responses of 37 channels' were overlayed at the mean DC level before the trigger point (time 0). Shaded areas on the RMS data represent the range of 0 to 40fT. The onset or offset of coherent motion occurred at time 0. Speed of the motion is indicated in the middle of the figure. Note that the peak of the first component in the response is clearly present in the RMS, as indicated by the arrowhead. The peak latencies of the first components for the slowest speed in both onset and offset responses were longer than the other latencies.

Figure 13: Averaged waveforms of the magnetic responses and the RMS values to the onset (S-R) and offset (R-S) of random motion are shown for the same subject as in Fig. 12. Waveforms of the responses and the time course of the RMS values are essentially the same as those for coherent motion. The peak latencies in the motion offset with the slowest speed was longer than the other latencies, but there was no latency change in the onset responses.

Figure 14: Peak latency changes in the first components of the magnetic responses in the first session for five subjects. The left graphs show latency changes in the responses to the onset (upper) and offset (lower) of coherent motion and the right graphs show latency changes for random motion. A significant effect of speed for the latency changes except for random motion onset was found by a two-factor ANOVA (subject and speed), as indicated by the P values. The post-hoc test (Bonferroni) showed that latencies for the responses at the speed of 0.6° s^{-1} were significantly longer than those for other speeds under all three stimulus conditions. Pairwise comparison of the latencies of onset and offset for each motion type with Bonferroni adjustment showed a significant difference ($P<0.05$) for the speeds of 9.6 and 25° s^{-1}.

Figure 15: Averaged waveforms of the magnetic responses and the RMS values to the change from random to coherent motion in the second session are shown for the same subject as in Fig. 12. Waveforms of the responses and the time course of the RMS values are essentially the same as those for coherent and random motion onset and offset. The stimulus condition is indicated at the left side. For example, C(0.6) →R(0.6) shows that the waveforms and RMS are for the responses to motion change from coherent motion at a speed of 0.6° s^{-1} to random motion at a speed of 0.6° s^{-1}. The peak latencies at the slowest speed (0.6° s^{-1}) of random motion were longer than the others, and the speed of subsequent motion did not affect the latencies.

Figure 16: Averaged waveforms of the magnetic responses and the RMS values to the change from coherent to random motion in the second session are shown for the same subject as in Fig. 12. Waveforms of the responses and the time course of the RMS values are essentially the same as those for coherent and random motion onset

and offset. The peak latencies at the slowest speed (0.6° s^{-1}) of coherent motion were longer than the others, and the speed of subsequent motion did not affect the latencies.

Figure 17: Changes in the peak latencies of the first response components of all the subjects and stimulus conditions used in the second session. For both types of change, a significant effect ($P<0.001$) was found for the speed of the preceding motion by a three-factor ANOVA (subjects, speed of preceding and subsequent motions).

Figure 18: The effect of stimulus conditions on the latency with varied preceding motion speed. Because the latencies changed only with the speed of preceding motions for the responses to the motion type changes, the averaged latency value across three responses of the same speed of preceding motion was used. Mean ± S.D. across all subjects' data are plotted with each speed of preceding motion in the graph. For the preceding motion, we compared between three graphs (see also Fig. 17) and they show that the peak latencies at the lowest speed (0.6° s^{-1}) of the preceding motion in all the four stimulus conditions are longer than the others. Two-factors ANOVA (subjects and stimulus conditions) did not reveal any significant difference in the latencies among four stimulus conditions (C-S, R-S, C-R, and R-C) for all three speeds.

Figure 19: Peak RMS values and ECD moments (M) (mean±S.D. across all the subjects' data) of the first components under all the stimulus conditions used in the first session. Both of these parameters significantly differed among the subjects, but there was no significant change for the stimulus conditions (P>0.05, two-factors ANOVA).

Figure 20: Peak RMS values and ECD moments (M) (mean±S.D. across all the subjects' data) of the first components under all the stimulus conditions used in the second session. Both parameters significantly differed among the subjects, but there was no significant effect for the stimulus conditions (P>0.05, three-factors ANOVA).

Figure 21: Effect of presence of the subsequent motion on the values of RMS and ECD moment (M) was checked with their mean values for each subject. For C-S, data for C(0.6)-S, C(9.6)-S, and C(25)-S were used to average. Similarly nine data were used to get mean value of C-R for each subject. No significant difference of both RMS and ECD moment between C-S and C-R, between R-S and R-C were found by paired t-test.

Figure 22: The coordinate system of the human brain. The origin of the coordinate system is the midpoint between the left and right PA points. The positive X-axis extends from the origin through the nasion. The positive Z-axis extends from the origin through the top of the head, such that it is perpendicular to the plane formed by the nasion and both PA points. The positive Y-axis extends from the origin through the left PA such that it is perpendicular to the X and Z axes.

Figure 23: Estimated locations of the origins of the first components under all the stimulus conditions are shown for each subject (S10, S19, S29, S40 and S52). In the 30 responses obtained for each subject, 30, 16, 18, 20 and 29 data could be used to estimate the origin using the single ECD model. The mean coordinate and mean distance +2 S.D. from the mean coordinate to each estimated location are shown for the individual subject.

Figure 24: Mean dipole location for each subject overlayed on the three dimensional brain images produced by MRI. Because the estimated location usually was in the sulcus, the nearest cortical surface in shown by a red dot.

Figure 25: The response latencies for all the subjects are plotted for each preceding motion speed. Note that the preceding speed 0 indicates the stationary dots and the responses included are onset responses to both coherent and random motions. As shown, there are two latency data distributions corresponding to the preceding motion speeds. The slow response group includes responses at slow preceding motion speeds (0 and 0.6° s^{-1}), and the fast response group does responses at fast preceding motion speeds (9.6 and 25° s^{-1}) (see also Table 3).

Figure 26: Distribution of the estimated dipole locations for slow (open circle) and fast (closed circle) response groups for each subject. Data are plotted as in Figure 23. Each subject's mean coordinate for each group's location is shown. All the subjects have the estimated locations for the slow responses that are distributed more laterally (right side, Y axis) than those for the fast responses. Their mean Y values are indicated by the closed (fast response group) and open (slow response group)

triangles.

Figure 27: Schematic illustration of the distribution of the estimated origins of the responses for each subgroup. Origins of the fast responses are located medial to the slow responses. In the fast response group, offset responses are estimated to originate anterior to those of the motion type changes. There was no significant difference in the estimated locations of coherent and random motions for the subgroups in the fast response group. In the slow response group, onset responses to random motion (R-on) were estimated to originate more medially than the onset responses to coherent motion (C-on). The origin of the response to the change from coherent to random motion (C-R) was located more medial compared to that of the change from random to coherent motion (R-C).

Figure 28: Changes in the peak RMS latencies of the onset and offset response to both coherent and random motions for a subject S52. Both offset response latencies were inversely related to the preceding motion speeds, whereas onset response latencies were not. Random motion with slower speeds was not as effective to the latency change as coherent motion.

11. Figures

Fig. 1

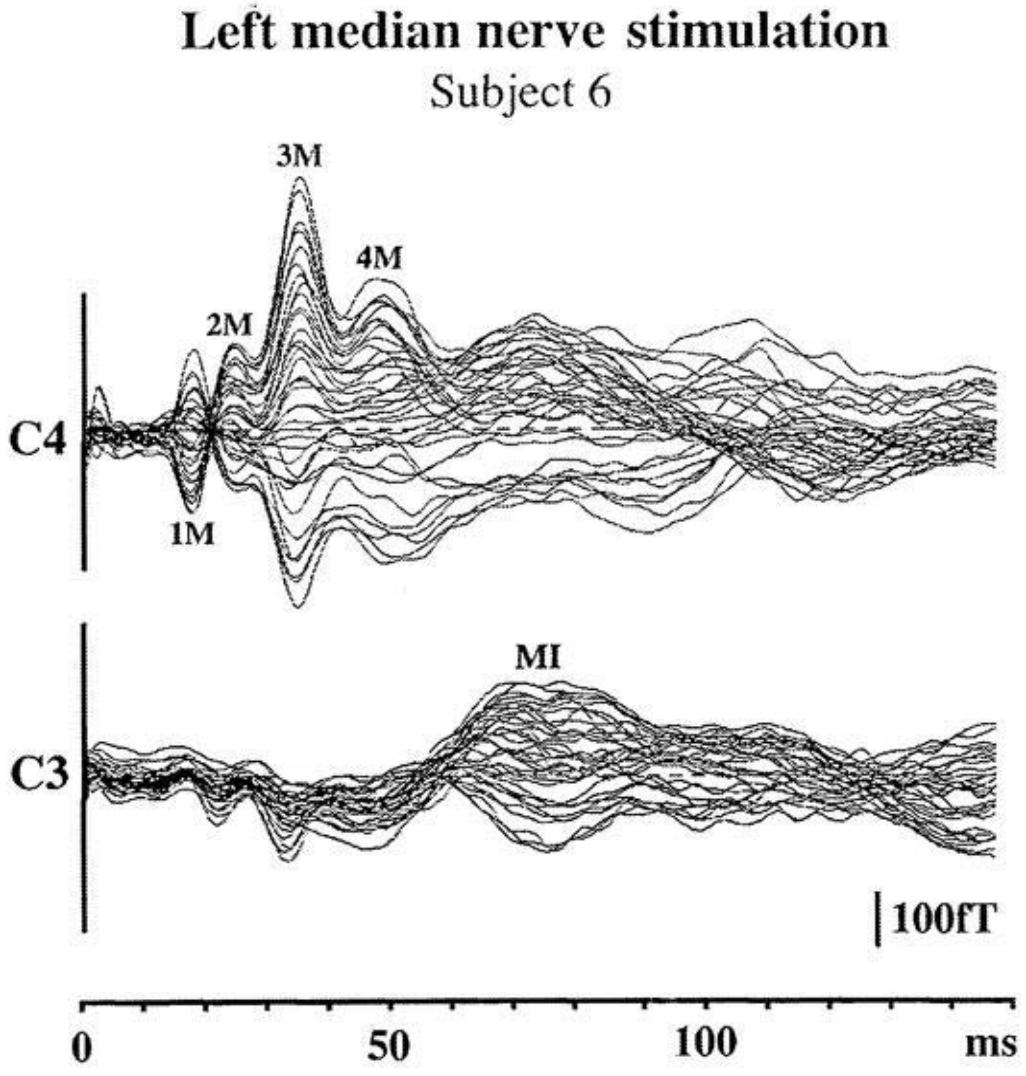

Fig. 2

Left median nerve stimulation (C4)

1M (17.3ms), Control, Subject 6

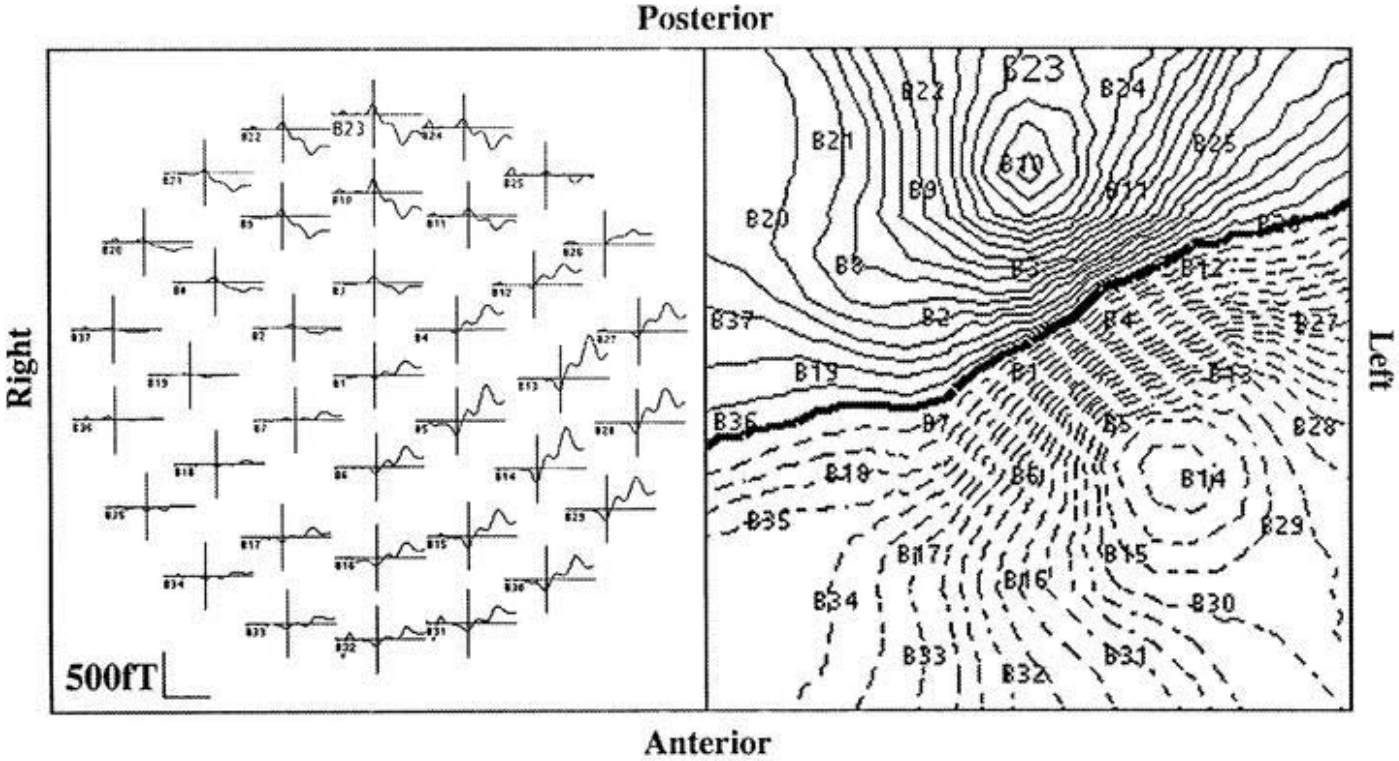

Fig. 3

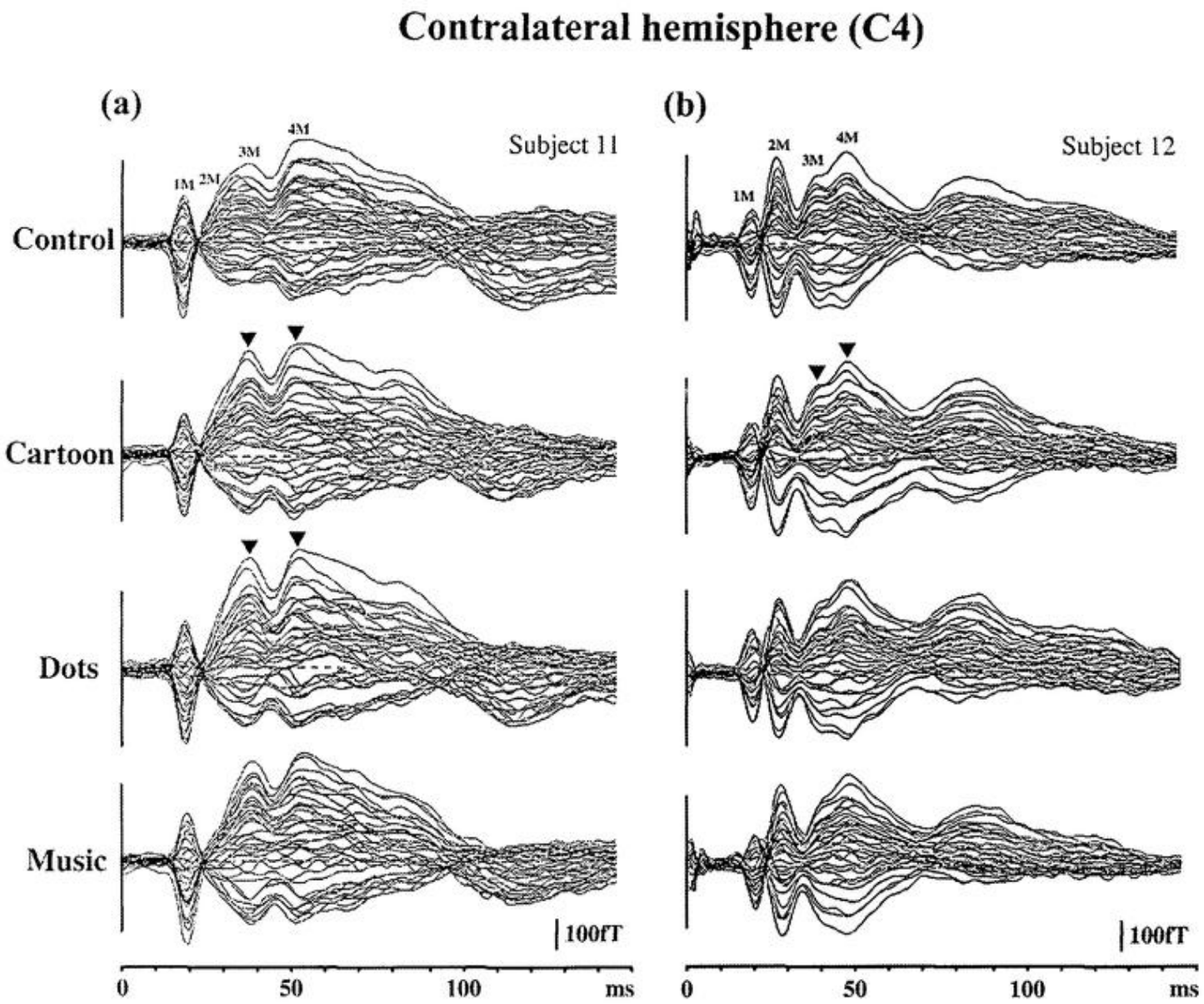
Contralateral hemisphere (C4)
(a)
Subject 11
1M
2M
3M
4M
Control
Cartoon
Dots
Music
100fT
0
50
100
ms
(b)
Subject 12
1M
2M
3M
4M
100fT
0
50
100
ms

Fig. 4

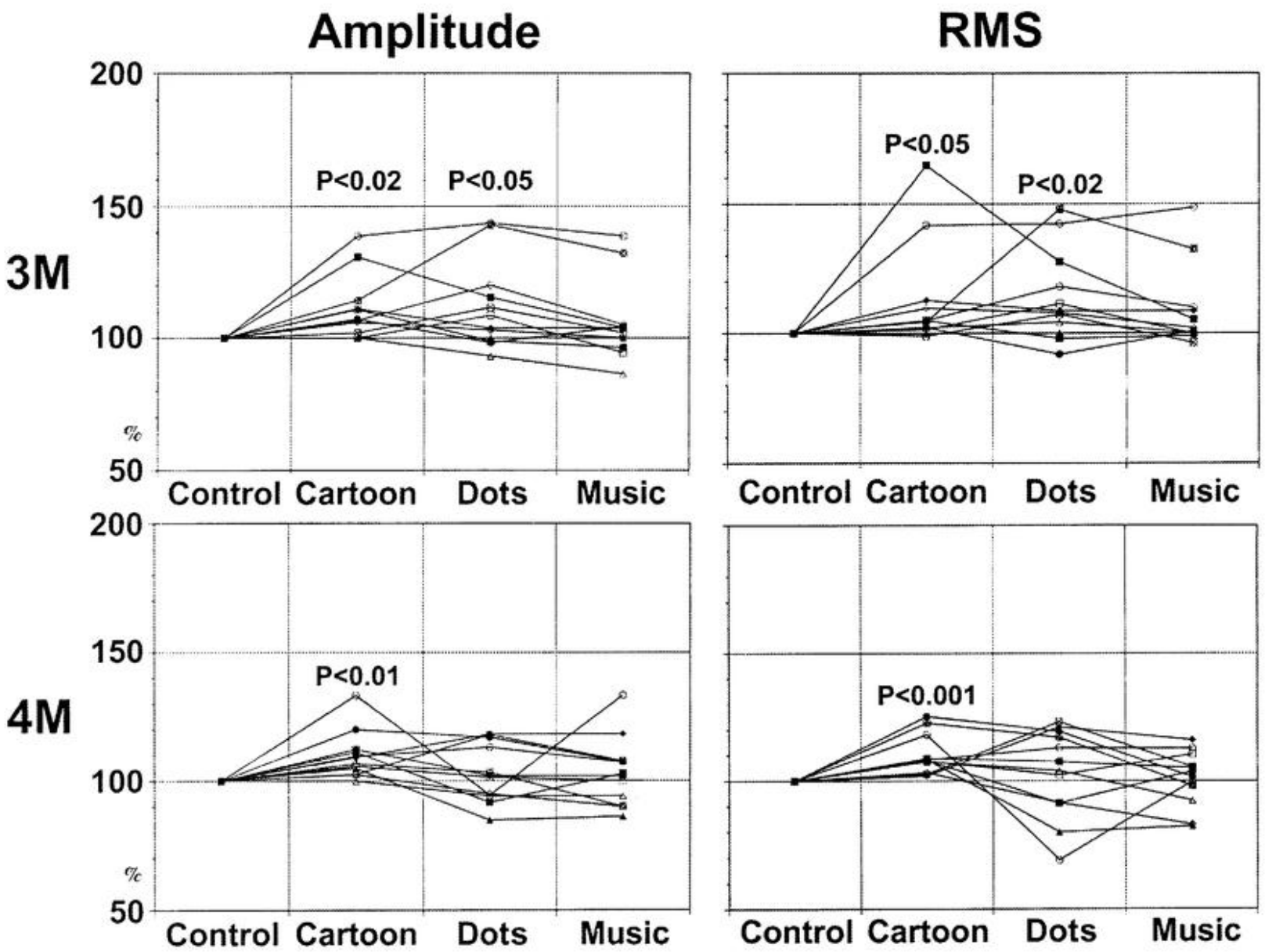
Amplitude
RMS
3M
4M
200
150
100
50
%
P<0.02
P<0.05
P<0.05
P<0.02
P<0.01
P<0.001
Control
Cartoon
Dots
Music

Fig. 5

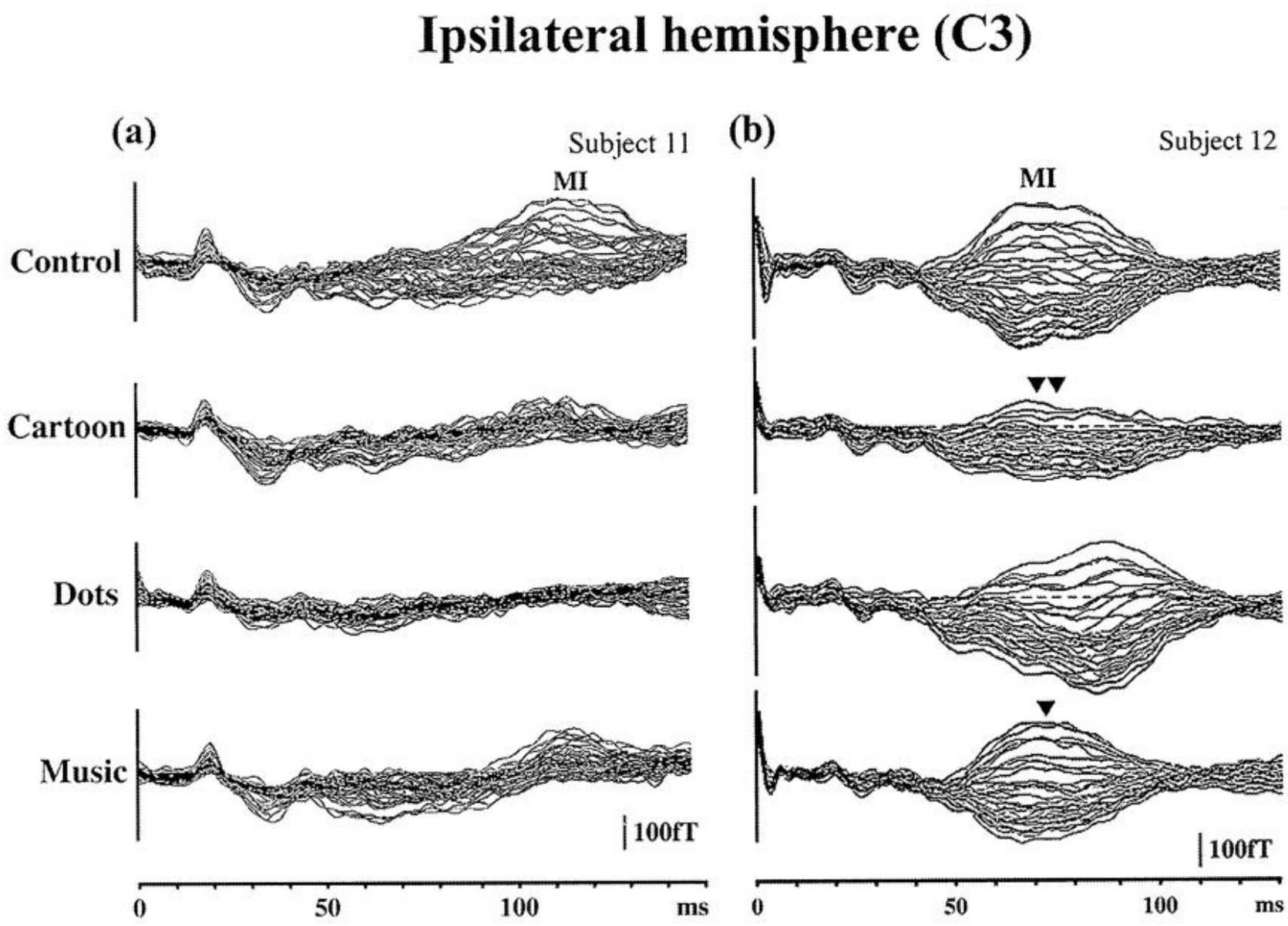
Ipsilateral hemisphere (C3)
(a)
Subject 11
MI
Control
Cartoon
Dots
Music
100fT
0
50
100
ms
(b)
Subject 12
MI
100fT
0
50
100
ms

Fig. 6

1M(17.3ms), Subject 6 , C4 position

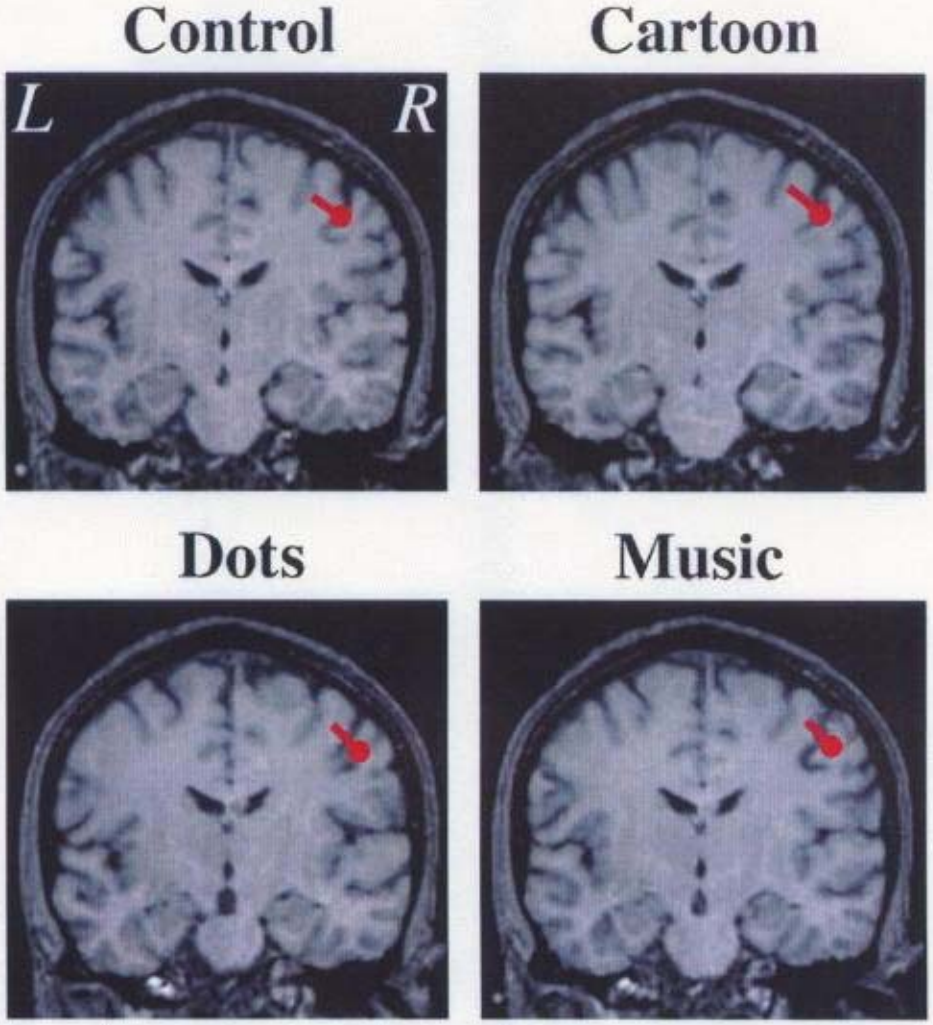

Fig. 7

3M (38.9 ms), Subject 12, C4 position

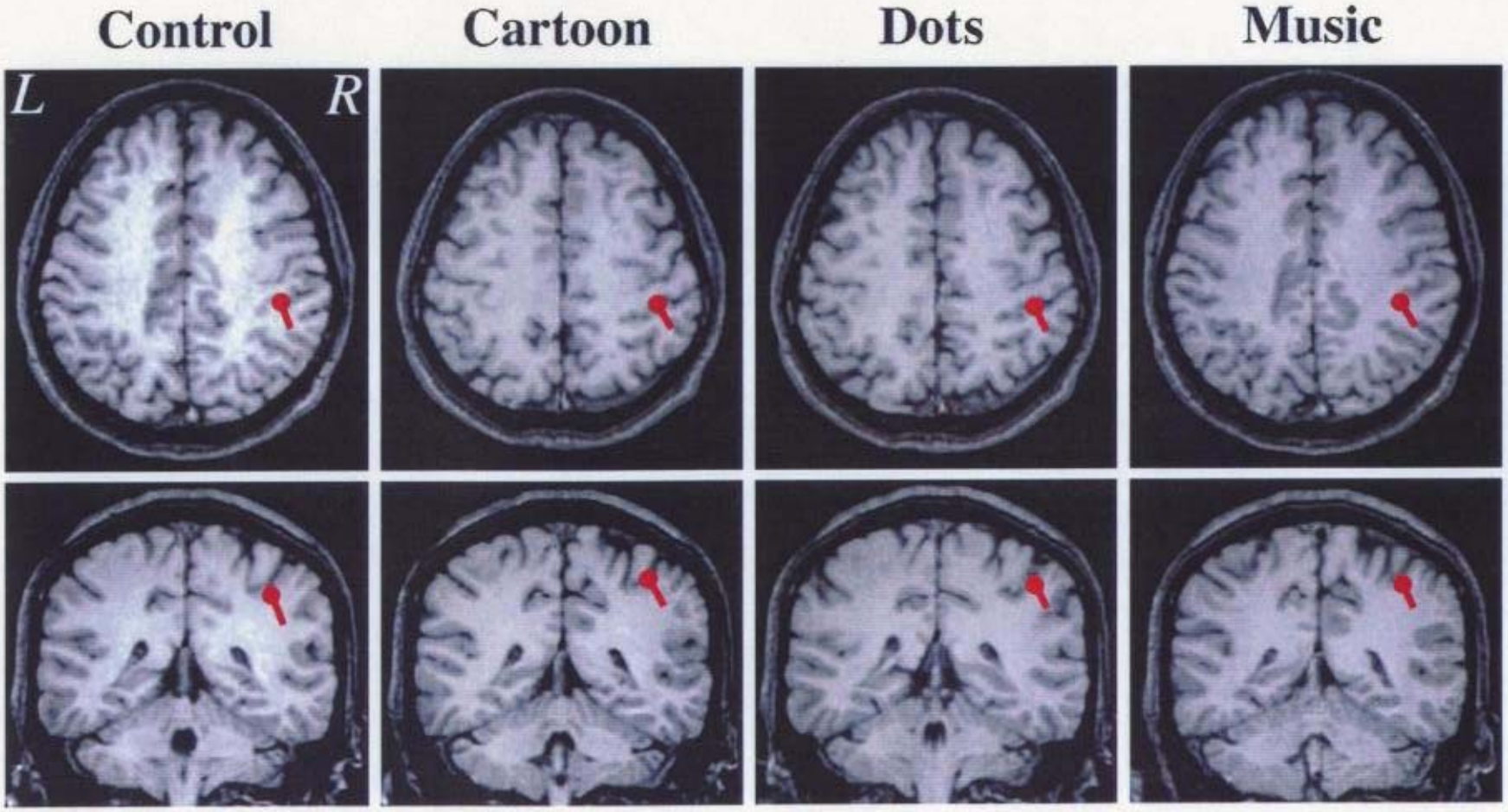

Fig. 8

4M (47 ms), Subject 12, C4 position

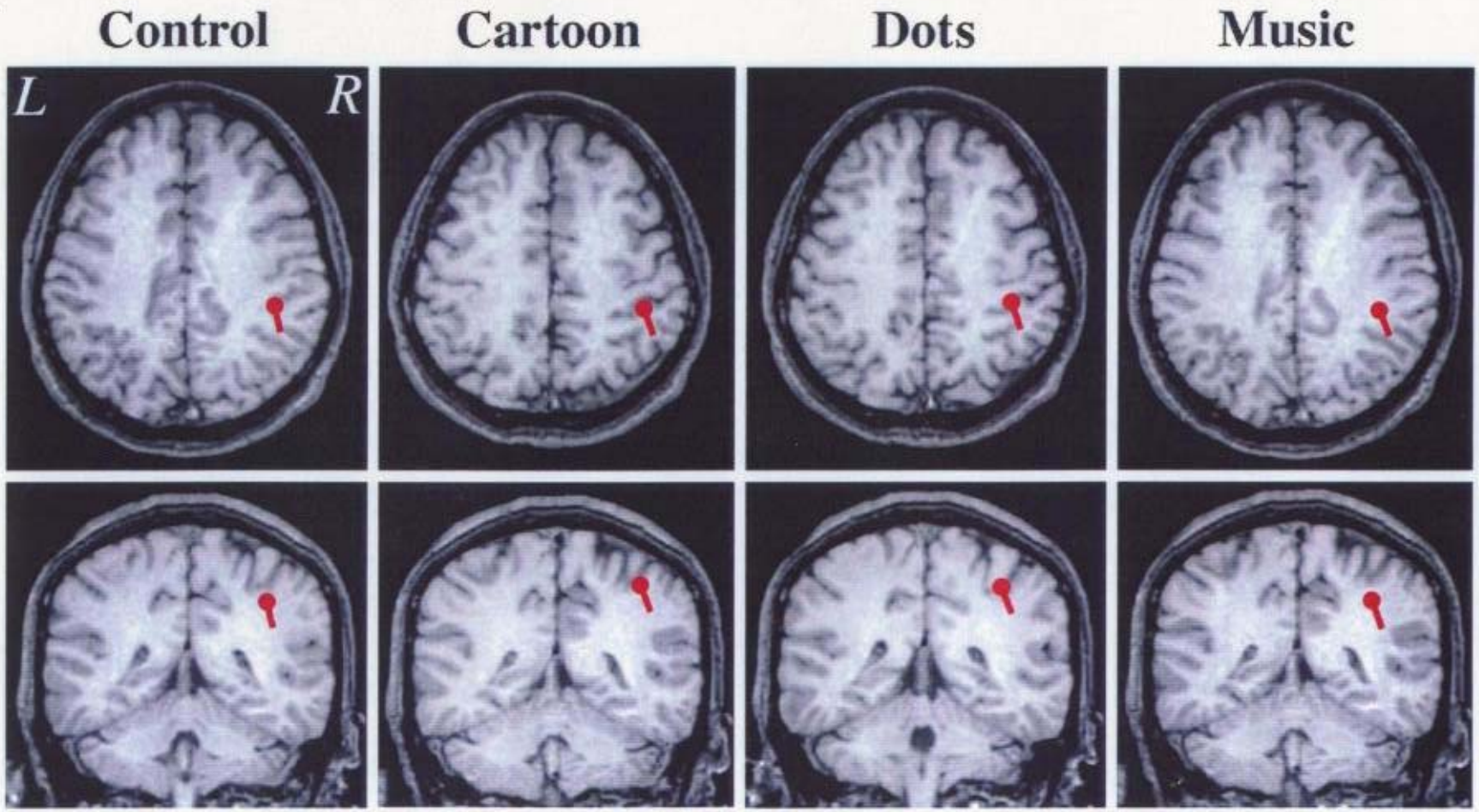

Fig. 9

MI, Subject 12, C3 position

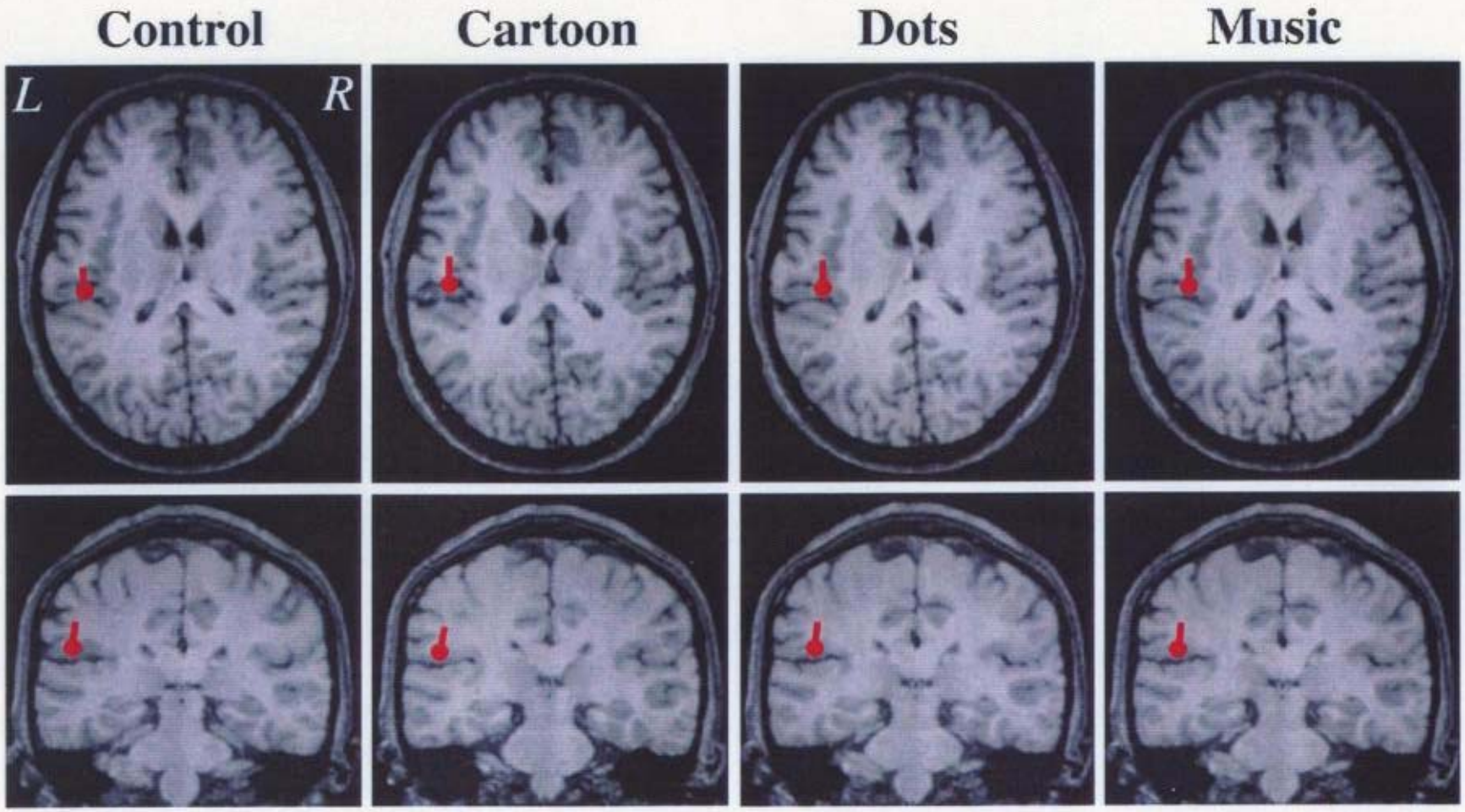

Fig. 10

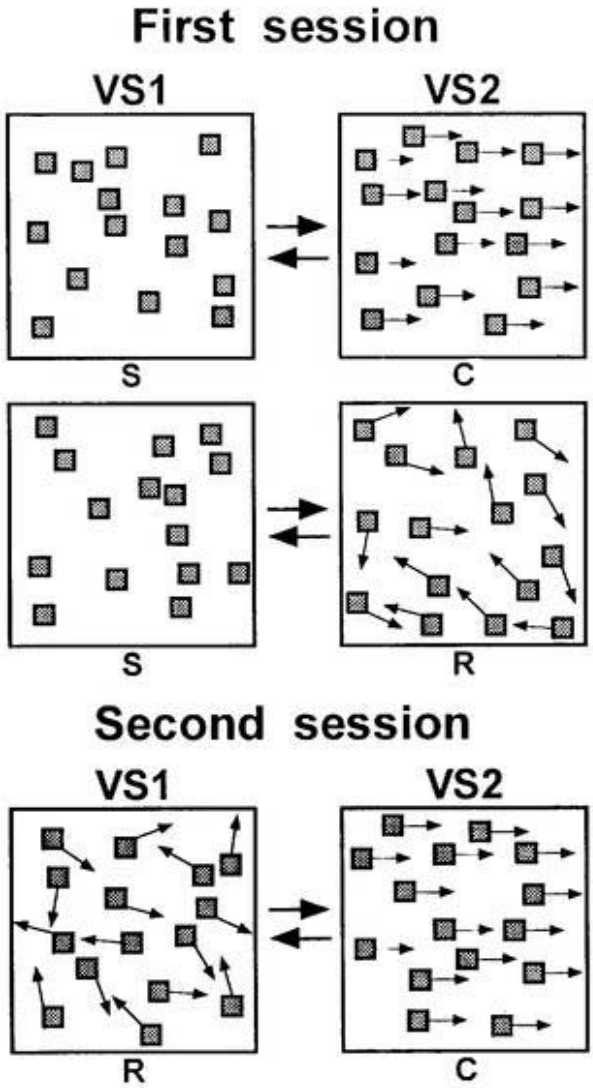

Fig. 11

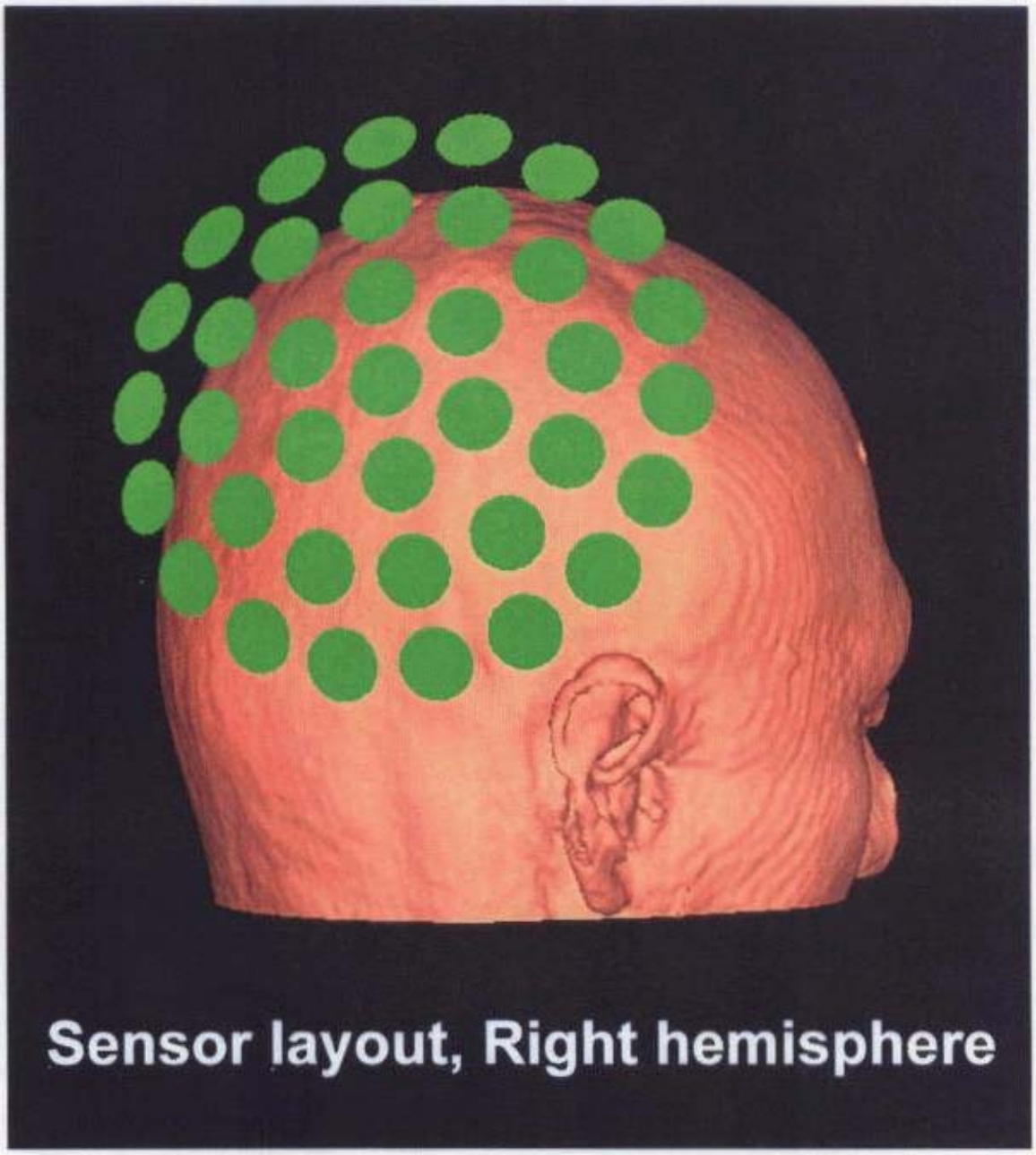

Fig. 12

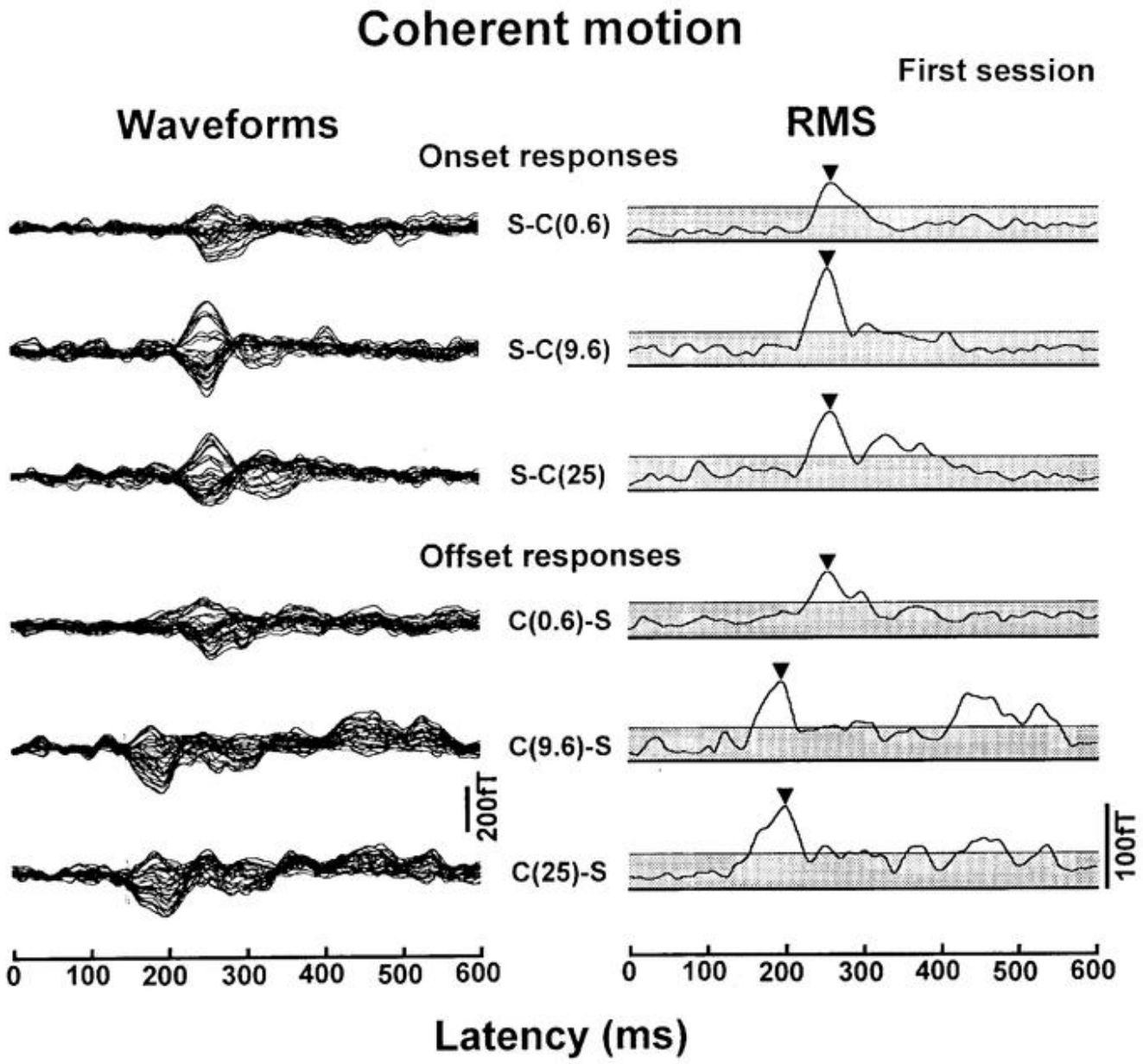
Coherent motion
First session
Waveforms
RMS
Onset responses
S-C(0.6)
S-C(9.6)
S-C(25)
Offset responses
C(0.6)-S
C(9.6)-S
C(25)-S
200fT
100fT
0 100 200 300 400 500 600
0 100 200 300 400 500 600
Latency (ms)

Fig. 13

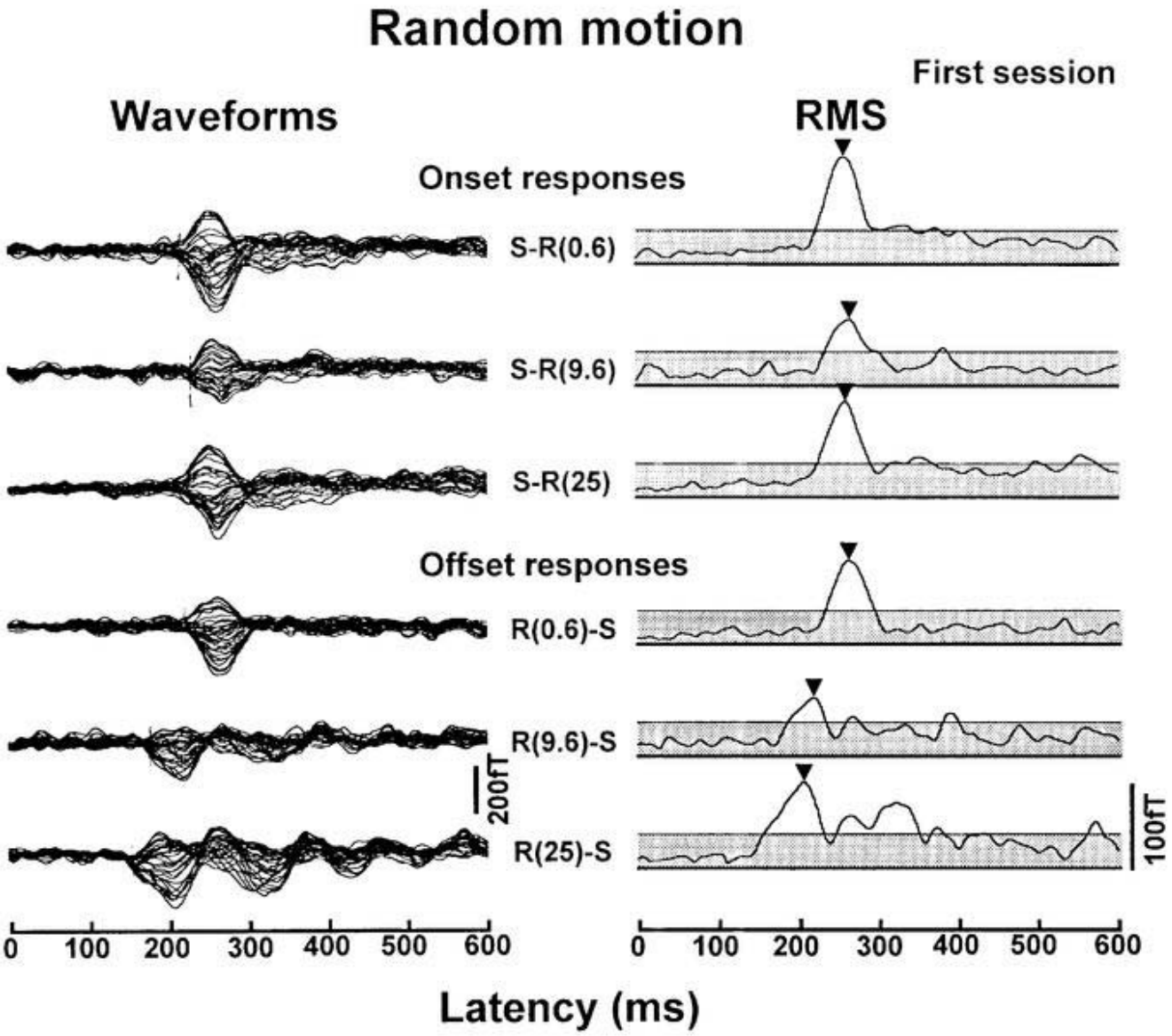
Random motion
First session
Waveforms
RMS
Onset responses
S-R(0.6)
S-R(9.6)
S-R(25)
Offset responses
R(0.6)-S
R(9.6)-S
R(25)-S
200fT
100fT
0
100
200
300
400
500
600
Latency (ms)

Fig. 14

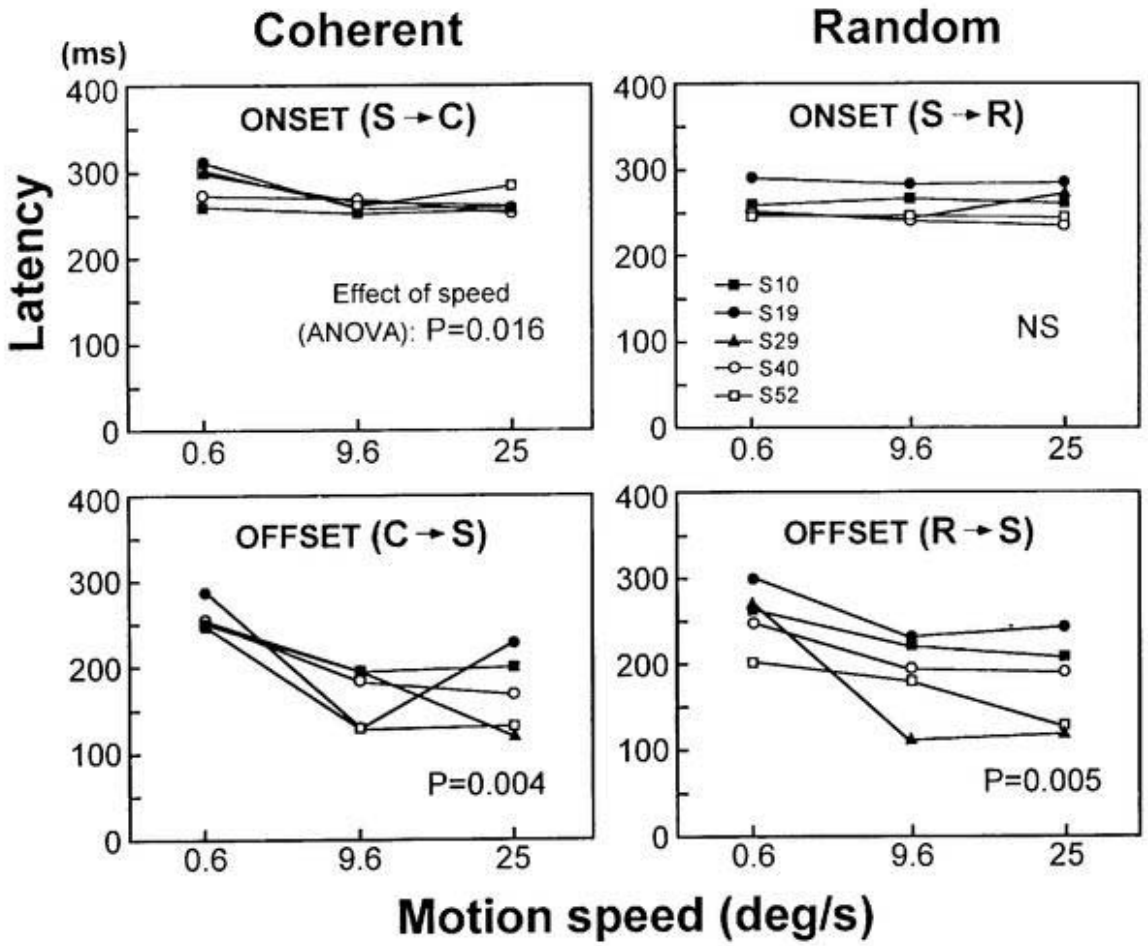
Coherent
Random
(ms)
Latency
ONSET (S → C)
Effect of speed
(ANOVA): P=0.016
ONSET (S → R)
S10
S19
S29
S40
S52
NS
OFFSET (C → S)
P=0.004
OFFSET (R → S)
P=0.005
400
300
200
100
0
0.6
9.6
25
Motion speed (deg/s)

Fig. 15

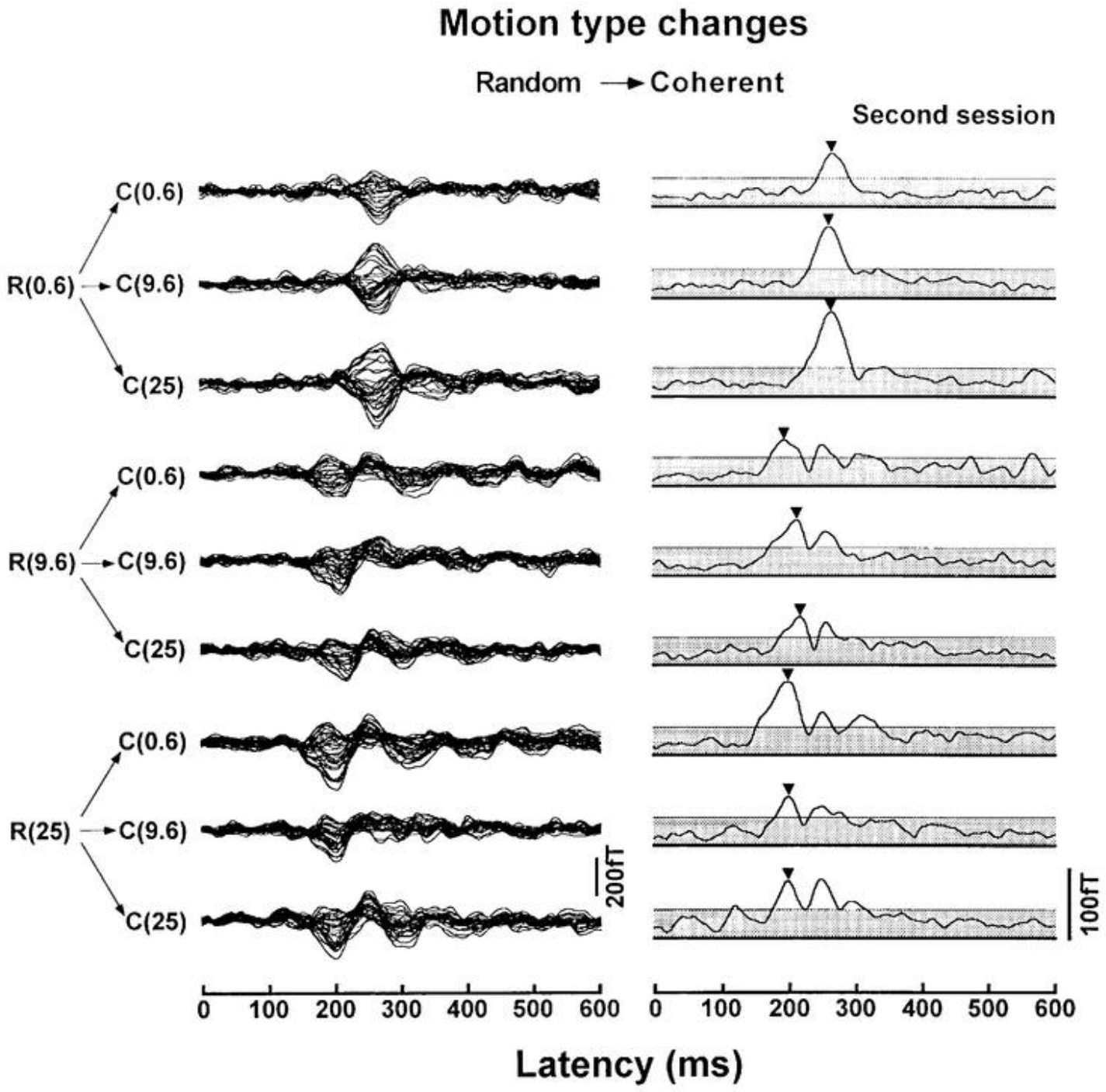
Motion type changes
Random → Coherent
Second session
R(0.6)
C(0.6)
C(9.6)
C(25)
R(9.6)
C(0.6)
C(9.6)
C(25)
R(25)
C(0.6)
C(9.6)
C(25)
200fT
100fT
0 100 200 300 400 500 600
0 100 200 300 400 500 600
Latency (ms)

Fig. 16

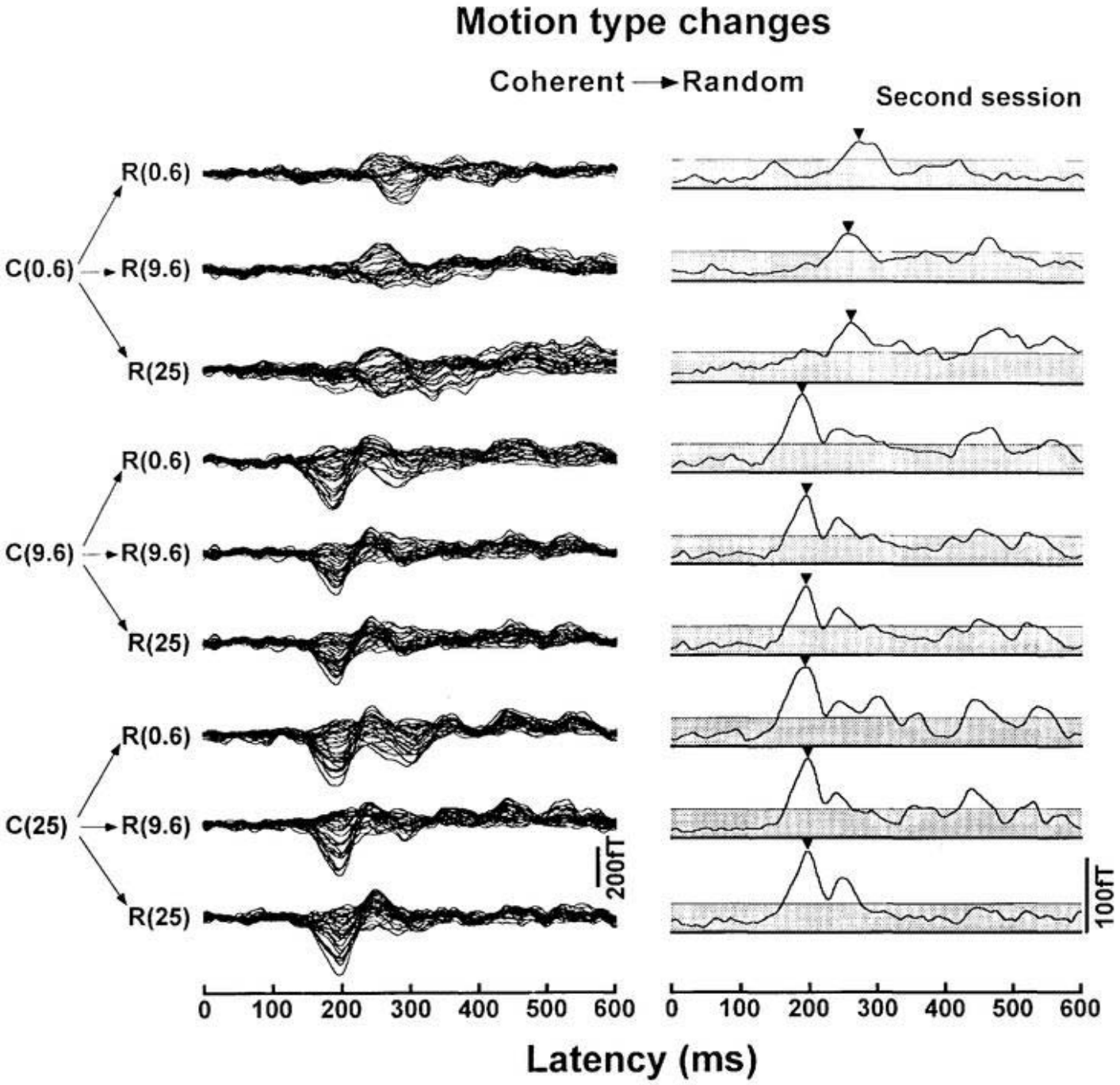
Motion type changes
Coherent → Random
Second session
R(0.6)
C(0.6)
R(9.6)
R(25)
R(0.6)
C(9.6)
R(9.6)
R(25)
R(0.6)
C(25)
R(9.6)
R(25)
200fT
100fT
0 100 200 300 400 500 600
0 100 200 300 400 500 600
Latency (ms)

Fig. 17

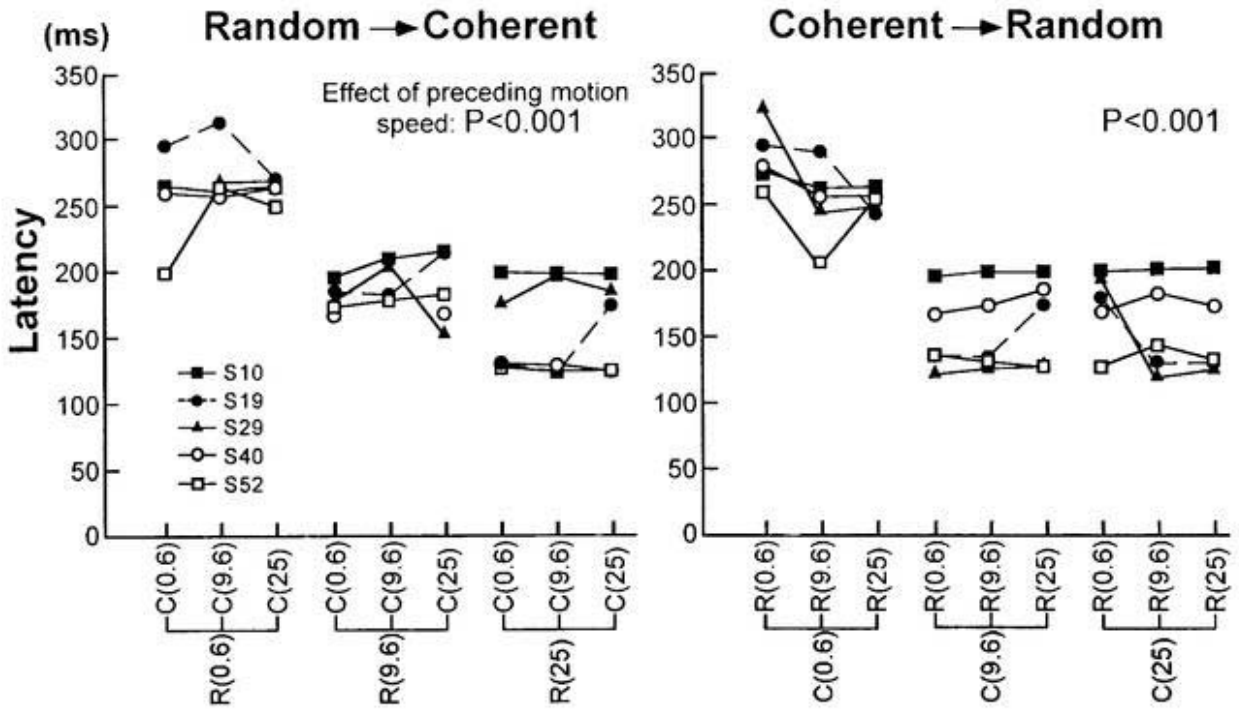
(ms)
Random → Coherent
Coherent → Random
Latency
Effect of preceding motion speed: P<0.001
P<0.001
S10
S19
S29
S40
S52
C(0.6)
C(9.6)
C(25)
R(0.6)
R(9.6)
R(25)

Fig. 18

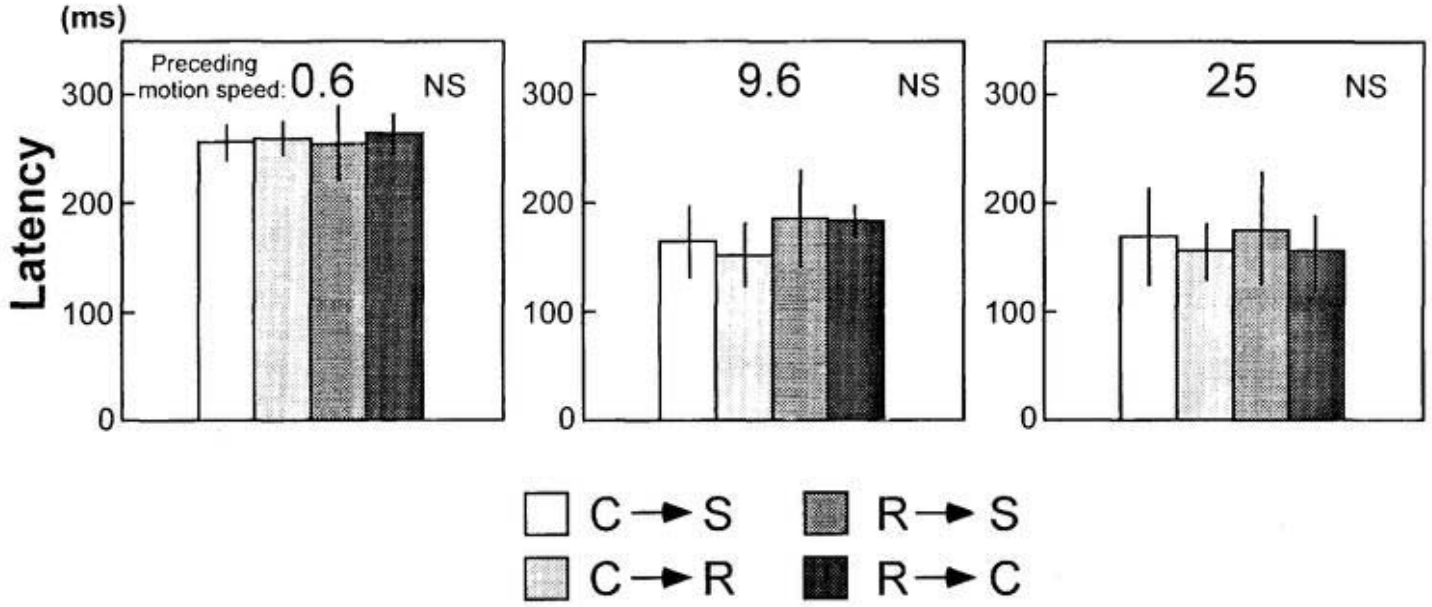
(ms)
Latency
Preceding motion speed:
0.6
9.6
25
NS
NS
NS
300
200
100
0
C→S
C→R
R→S
R→C

Fig. 19

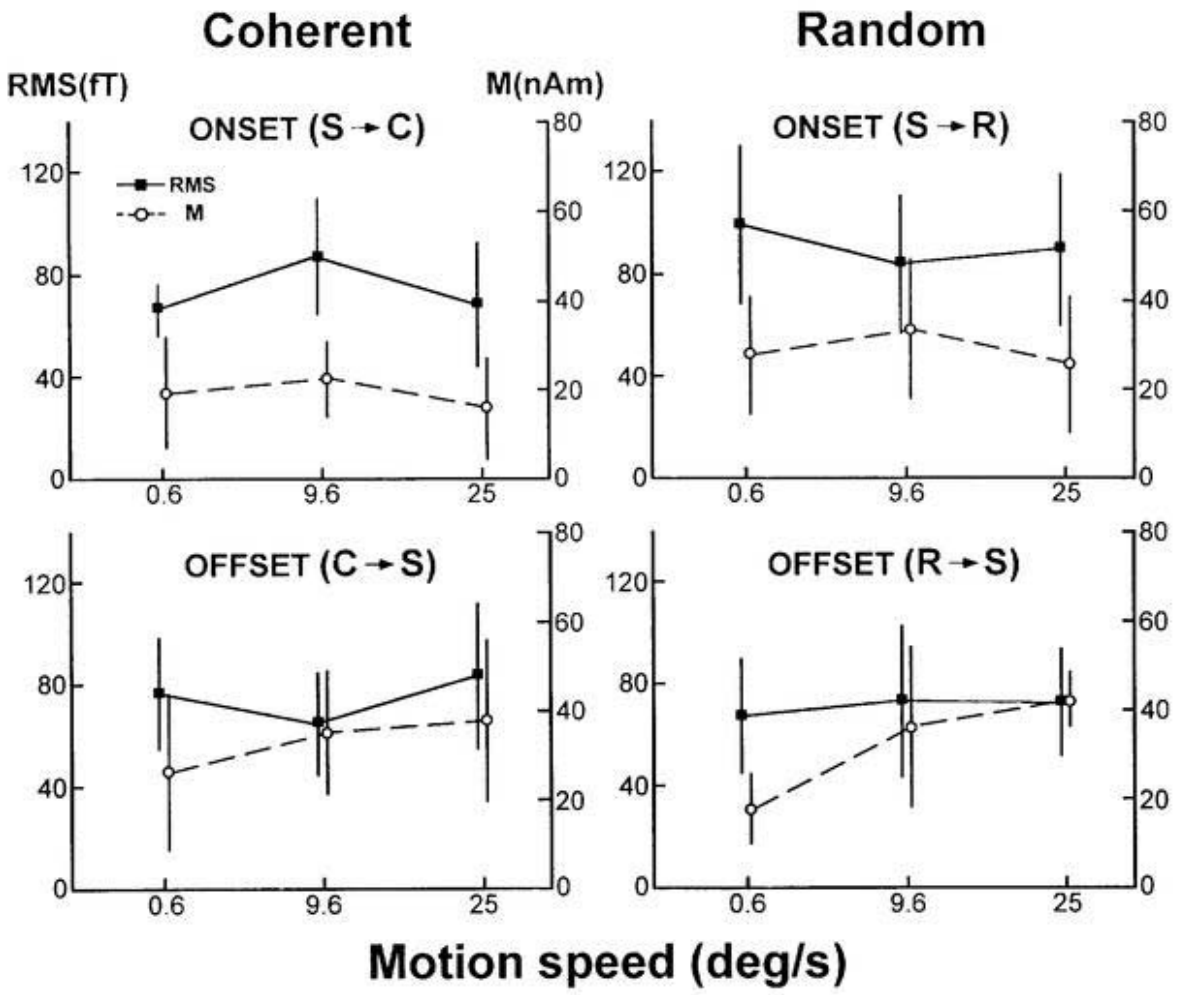
Coherent
Random
RMS(fT)
M(nAm)
ONSET (S → C)
ONSET (S → R)
OFFSET (C → S)
OFFSET (R → S)
RMS
M
120
80
40
0
60
20
0.6
9.6
25
Motion speed (deg/s)

Fig. 20

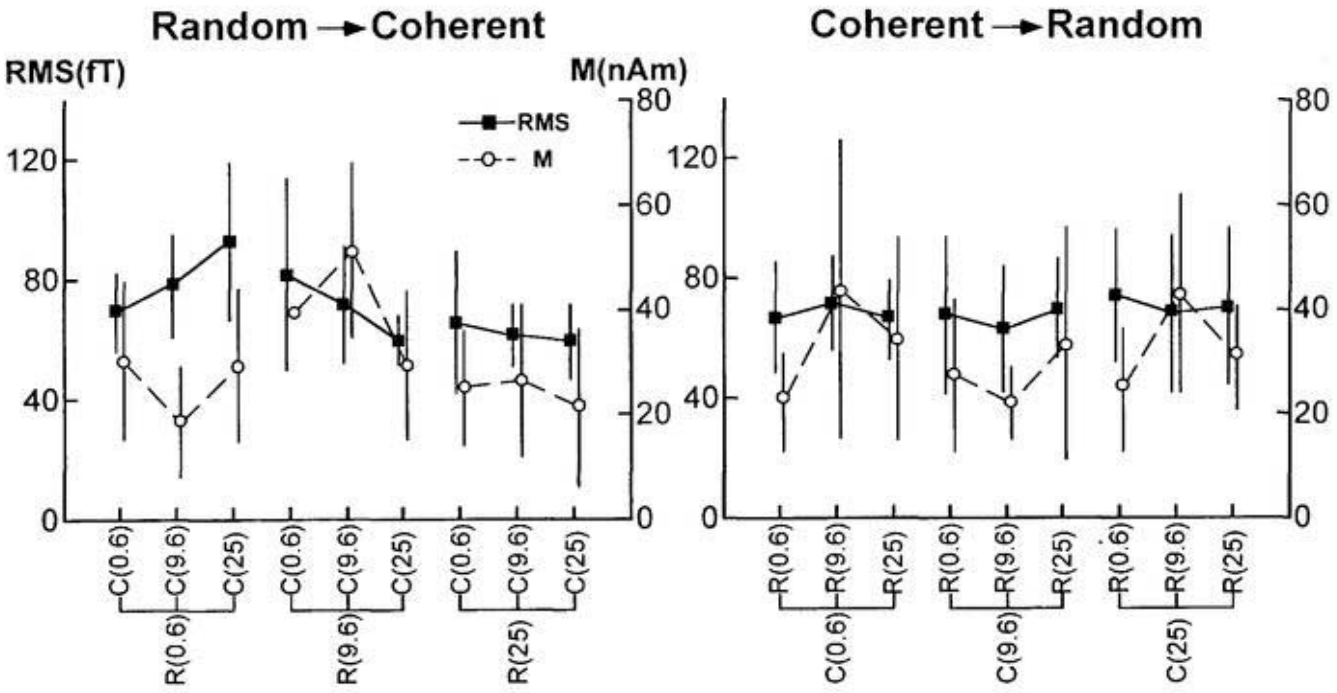
Random → Coherent
Coherent → Random
RMS(fT)
M(nAm)
RMS
M
120
80
40
0
60
20
C(0.6)
C(9.6)
C(25)
R(0.6)
R(9.6)
R(25)

Fig. 21

Effect of presence of the subsequent motion on RMS and dipole moment (M)

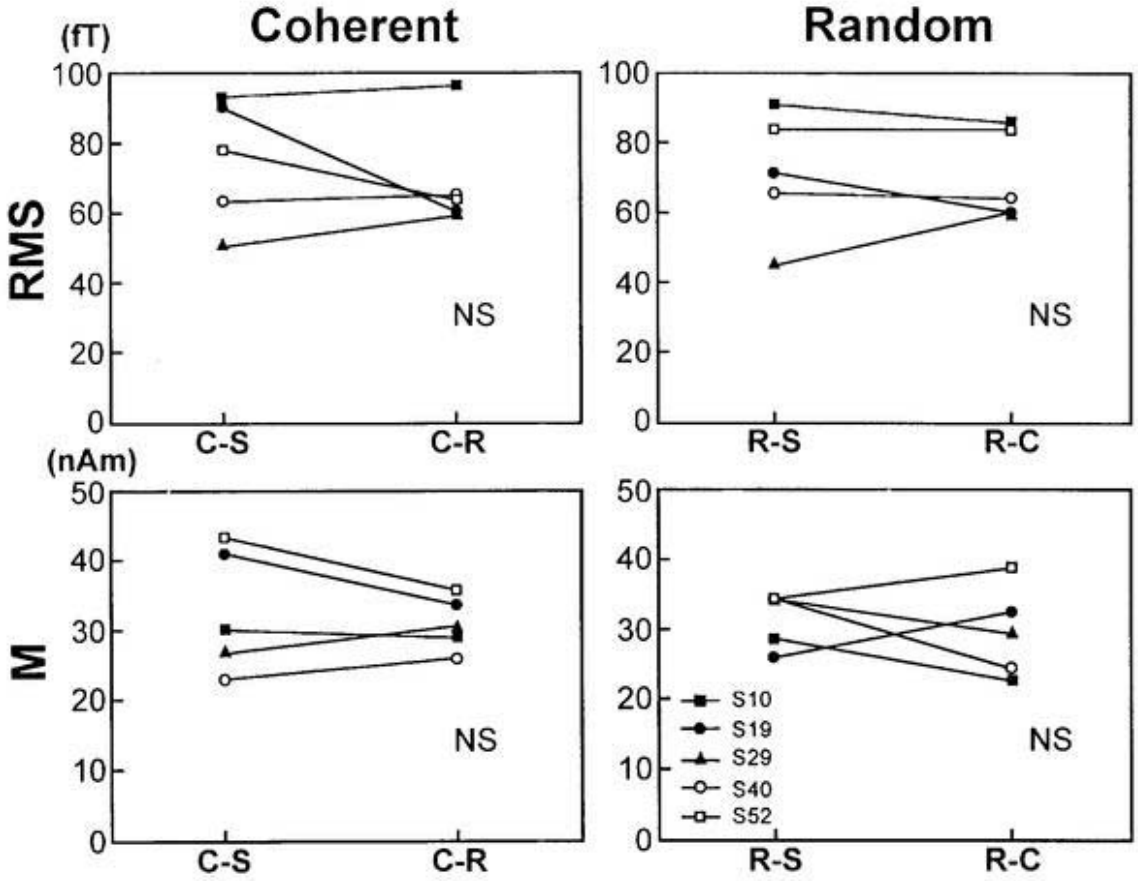

Fig. 22

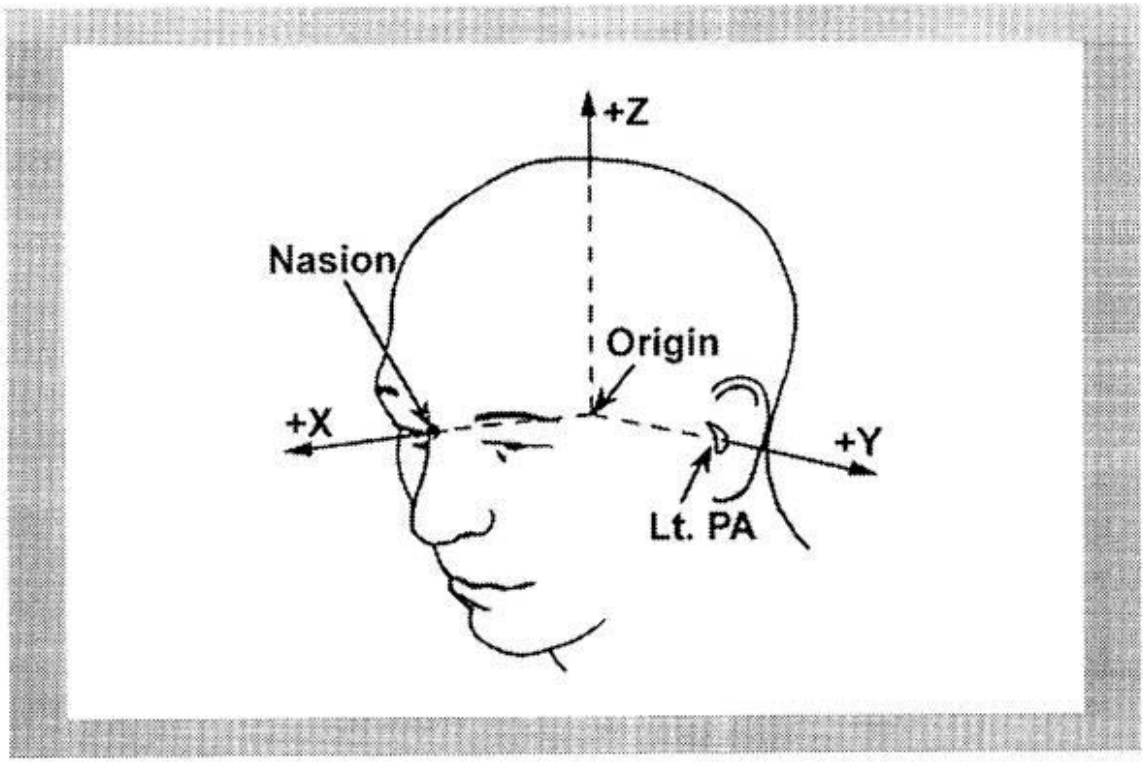

Fig. 23

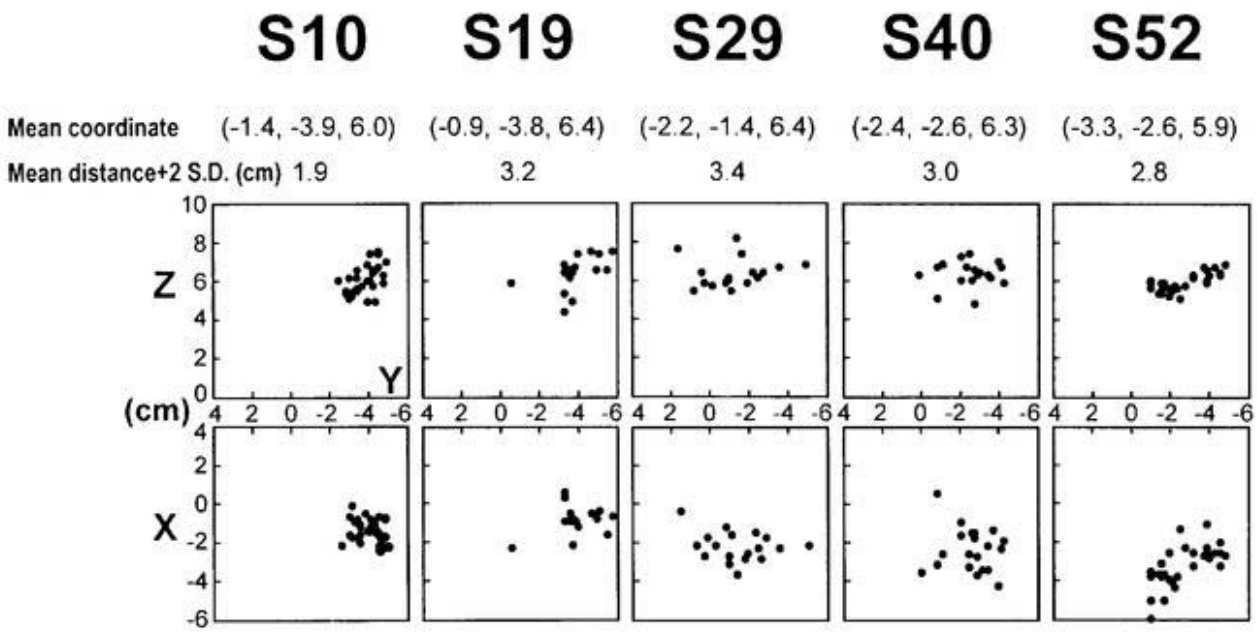
S10
S19
S29
S40
S52
Mean coordinate
(-1.4, -3.9, 6.0)
(-0.9, -3.8, 6.4)
(-2.2, -1.4, 6.4)
(-2.4, -2.6, 6.3)
(-3.3, -2.6, 5.9)
Mean distance+2 S.D. (cm)
1.9
3.2
3.4
3.0
2.8
Z
Y
X
(cm)

Fig. 24

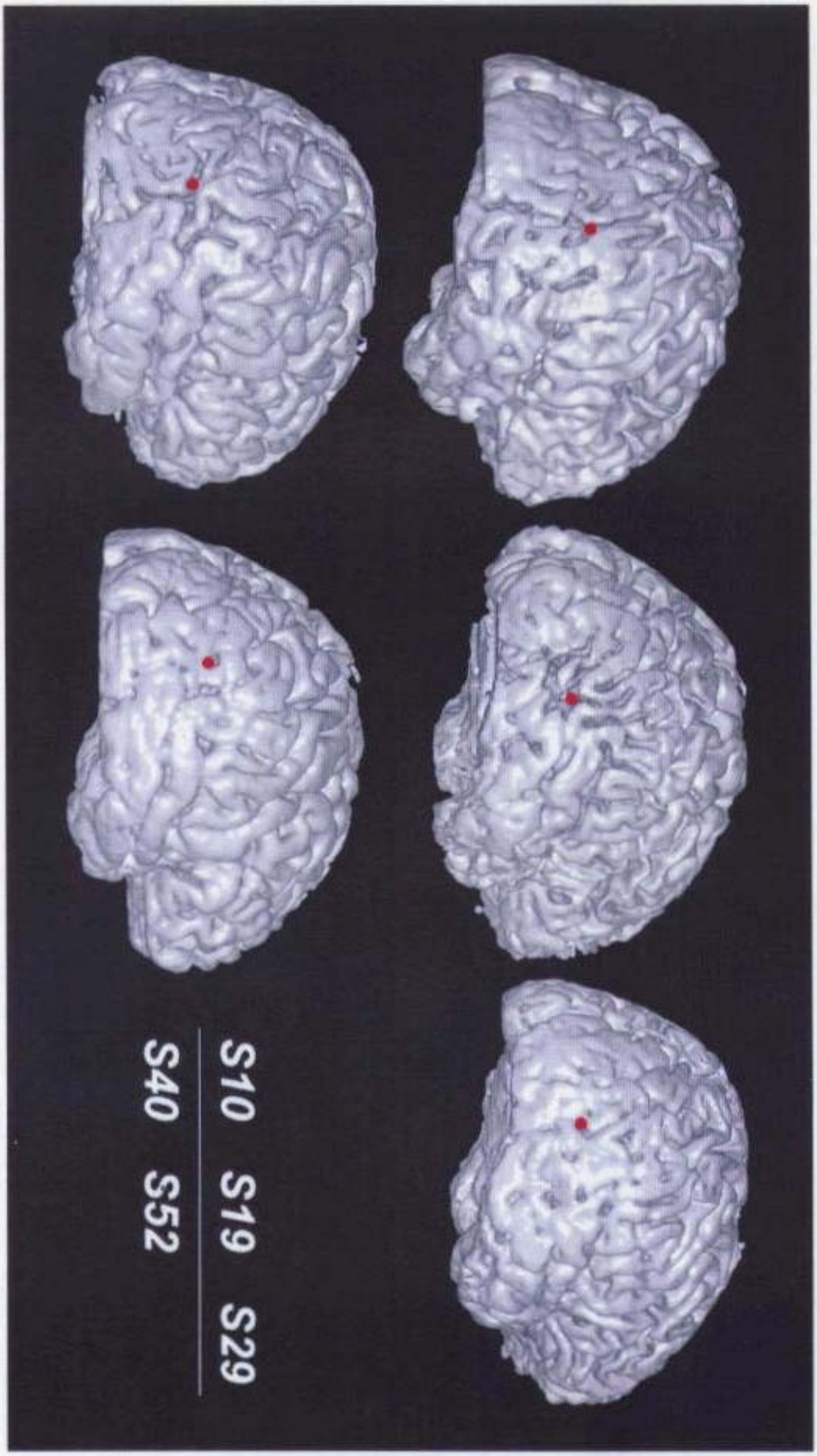

Fig. 25

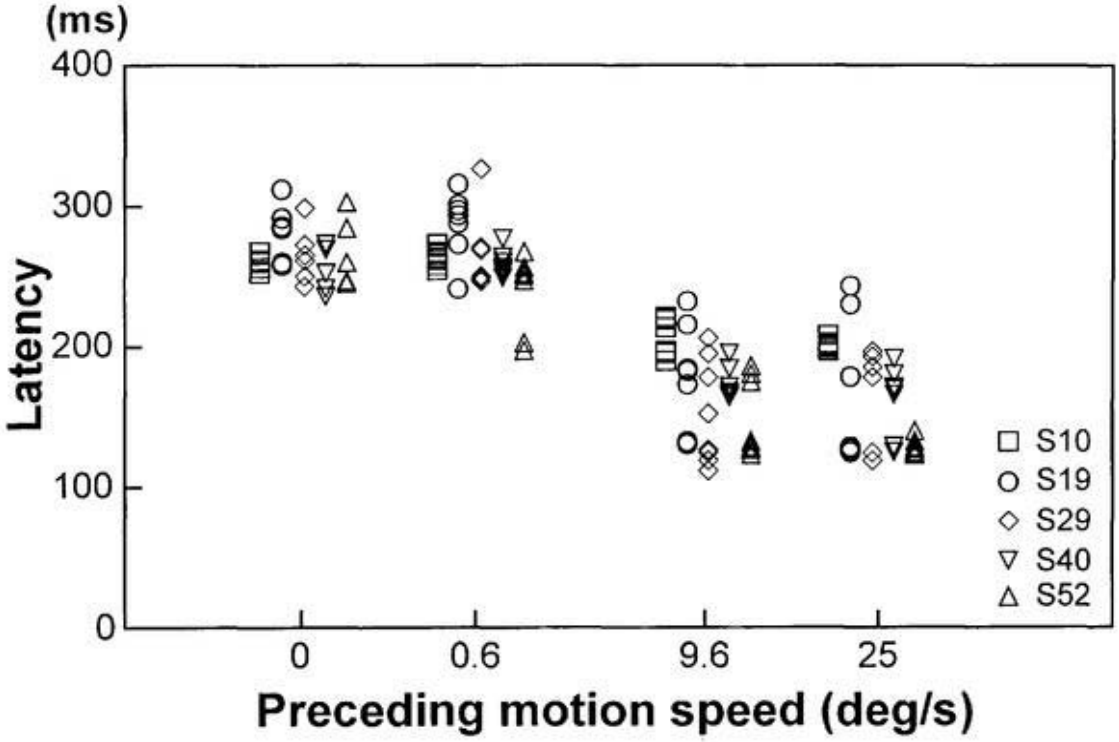
(ms)
400
300
200
100
0
Latency
0
0.6
9.6
25
Preceding motion speed (deg/s)
S10
S19
S29
S40
S52

Fig. 26

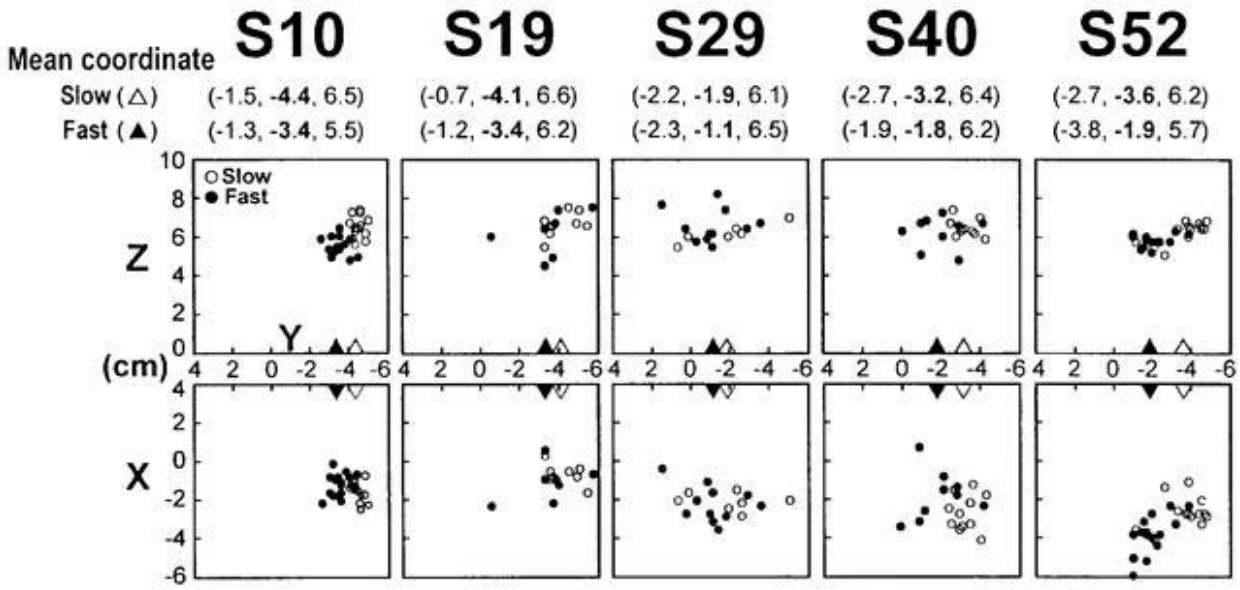
Mean coordinate
S10
S19
S29
S40
S52
Slow (△)
(-1.5, -4.4, 6.5)
(-0.7, -4.1, 6.6)
(-2.2, -1.9, 6.1)
(-2.7, -3.2, 6.4)
(-2.7, -3.6, 6.2)
Fast (▲)
(-1.3, -3.4, 5.5)
(-1.2, -3.4, 6.2)
(-2.3, -1.1, 6.5)
(-1.9, -1.8, 6.2)
(-3.8, -1.9, 5.7)
○ Slow
● Fast
Z
Y
X
(cm)

Fig. 27

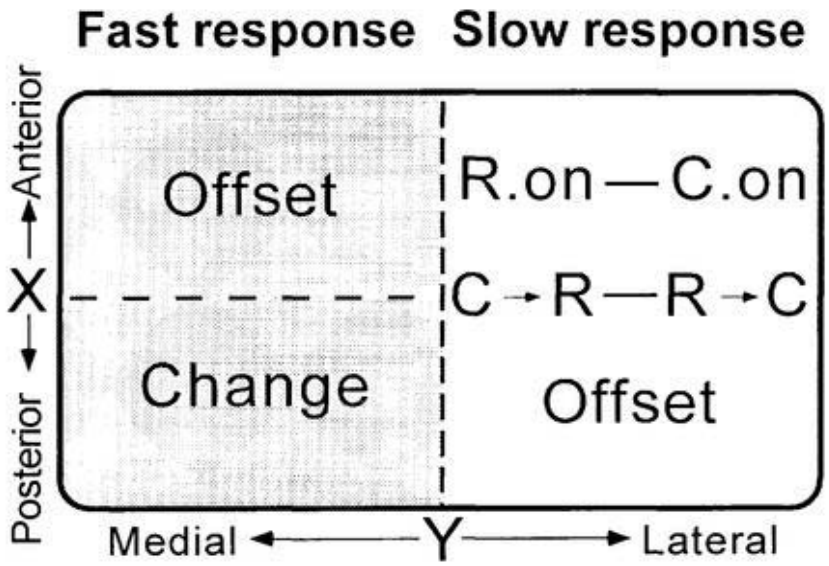
Fast response
Slow response
Anterior
Posterior
X
Offset
Change
R.on — C.on
C → R — R → C
Offset
Medial
Y
Lateral

Fig. 28

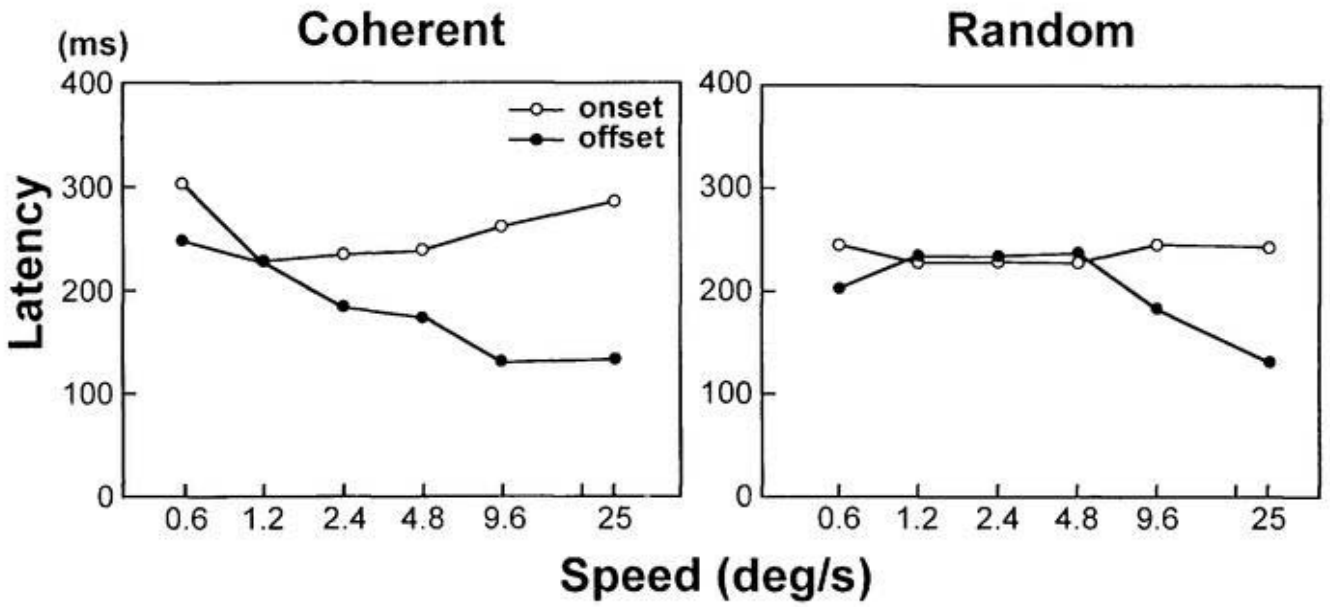
Coherent
Random
(ms)
Latency
400
300
200
100
0
onset
offset
0.6
1.2
2.4
4.8
9.6
25
Speed (deg/s)

12. Publications

Lam K, Kakigi R, Kaneoke Y, Naka D, Maeda K, Suzuki H (1999) Effects of visual and auditory stimulation on somatosensory evoked magnetic fields. Clin. Neurophysiol. **110**: 295-304.

Lam K, Kakigi R, Kaneoke Y, Naka D, Maeda K, Suzuki H (1998) Does continuos visual and auditory stimulation affect somatosensory evoked magnetic fields ? Recent Advances in Human Neurophysiology (Edited by Hashimoto I. and Kakigi R., Elsevier, Amsterdam): pp866-871.

Lam K, Kakigi R, Kaneoke Y, Naka D, Maeda K, Suzuki H (1999) The interference effects of continuos visual and auditory stimulation on somatosensory evoked magnetic fields. Proc. 11th Int. Conference on Biomagnetism (Edited by Yoshimoto T. et al., Tohoku University Press, Sendai), in press.

Lam K, Kaneoke Y, Gunji A, Yamasaki H, Matsumoto E, Naito T and Kakigi R. Response of the human extrastriate cortex in detection of coherent and incoherent motions, in submission.